THE DULCE, NEW MEXICO, EARTHQUAKE OF JANUARY 23, 1966: LOCATION, FOCAL MECHANISM, MAGNITUDE, AND SOURCE PARAMETERS

A Dissertation
Presented to the Faculty
of the New Mexico Institute of
Mining and Technology

In Partial Fulfillment
of the Requirements for the
Degree of Doctor of Philosophy
in Geoscience

by
Daniel J. Cash

May 1971

ABSTRACT

The Dulce, New Mexico, earthquake of January 23, 1966, was studied, using the nuclear explosion, Gasbuggy, as a control in some of the analyses. Gasbuggy occurred on December 10, 1967, about 40 kilometers southwest of the earthquake epicenter.

The earthquake's origin time and coordinates were determined by subtracting the distance and time residuals for Gasbuggy from those for the earthquake. The results were an origin time of 01h 56m 39.3s GMT and coordinates of 36.96° north latitude and 106.95° west longitude.

The focal mechanism of the earthquake was determined from the first motion of the initial P phase on short-period records. The result of this study was that the earthquake probably occurred as a result of right-lateral strike-slip movement on a fault striking N18°W and dipping 79° ENE. Movement on the fault plunged 20° in a direction N14°W. The distinction between the fault plane and the auxiliary plane was based on geological considerations.

The magnitudes of the earthquake and the nuclear explosion were calculated from only those seismograms which yielded good amplitude data for both events. Three types of magnitude were considered: m, from the refracted P phase; m_6, from the direct P phase; and M_s, from surface

(Rayleigh) waves. The calculated average values of the magnitudes for the earthquake were m = 5.1, m_6 = 5.3, and M_S = 4.9. For Gasbuggy the values were m = 5.1, m_6 = 4.6, M_S = 4.3. The value of m was the same for both events, but m_6 and M_S were considerably larger for the earthquake than for the nuclear explosion. This difference reflects the difference in the source mechanisms and lends support to the strike-slip mechanism for the earthquake. The variation in the values of each type of magnitude from station to station was the same for both events. Therefore, the scatter in the calculated magnitude values for both seismic events was probably the result of variations in crustal and upper mantle structure.

The source durations of the Dulce earthquake and Gasbuggy were determined from the ratio of the amplitude spectra and were found to be 1.8 and 0.5 seconds, respectively. The radius of the nuclear explosion was calculated from the time duration to be 0.75 kilometers. Similarly, the linear source dimension of the earthquake was found to be 6.3 kilometers if the fault propagated unilaterally, and 12.6 kilometers if the fault propagated bilaterally. Fault dimensions calculated from magnitude m and the period of the largest Rayleigh wave were 16 and 12 kilometers, respectively. From relationships between fault dimension, displacement, and magnitude, the displacement during the earthquake was calculated to be about 1 centimeter.

ACKNOWLEDGEMENTS

I am much indebted to Dr. Allan R. Sanford, my advisor and committee chairman, for suggesting the topic for study and for being so generous with his time and assistance. Special thanks are due to Margie, my wife, for her encouragement and patience, as well as for her help in such matters as proofreading.

The other members of my committee also provided helpful suggestions in the writing of the dissertation. They are Dr. Antonius J. Budding, Dr. Leslie D. Fallon, and Dr. Alan Sharples.

Financial assistance for the research was provided by a National Science Foundation Science Faculty Fellowship.

TABLE OF CONTENTS

LIST OF FIGURES

LIST OF TABLES

1. INTRODUCTION

Significance of the Dissertation

On January 22, 1966, at 6:56 P. M. MST, a moderately damaging earthquake occurred in the vicinity of Dulce, New Mexico. U. S. Coast and Geodetic Survey (now National Ocean Survey) assigned the event a magnitude (m_b) of 5.5, a location of 37.0° north latitude and 107.0° west longitude, and an origin time of 01h 56m 38.8s GMT. (Von Hake and Cloud, 1968). The depth was arbitrarily taken to be 10 kilometers.

There are several reasons for investigating this relatively moderate strength earthquake. First, an earthquake of this magnitude could have been more serious if it had struck in an area of higher population density than Dulce. For example, a pair of earthquakes of about this magnitude (5.6 and 5.7) occurred on October 1, 1969, at Santa Rosa, California, doing damage to buildings estimated at six million dollars (compared to $200,000 at Dulce) (Steinbrugge et al., 1970). Steinbrugge et al. further estimated that a shock of this magnitude in San Francisco or Los Angeles could cause damage of 25 million dollars or more.

Second, earthquakes of this magnitude (m_b = 5.5 CGS) and maximum intensity (VII M. M.) are rare in the Southern Rocky Mountain region. Reports by Sanford (1965) and

Sanford and Cash (1969) show that between January 1, 1962, and December 31, 1967, the largest shock in New Mexico, other than those near Dulce, was one of magnitude 4.5 (m_b) near the New Mexico-Colorado border between Raton and Trinidad.

Richter (1959) lists 27 significant events or groups of events which have occurred in the U. S. outside of California and western Nevada between 1663 and 1954. Of these, the closest to Dulce was a group of shocks, in 1906, near Socorro, New Mexico, 300 kilometers south of Dulce. These last events had reported intensities as high as VIII (M. M.) (Sanford, 1963) and one was felt over an area of 100,000 square miles. The area of perceptibility indicates a shock of about magnitude 6.

The seismic history of Colorado shows that since 1944 (1) three shocks having maximum reported intensities of VI have occurred in southwest Colorado in the vicinity of Montrose, 200 kilometers northwest of Dulce, and (2) one of intensity V occurred in Conejos County, Colorado, just northeast of Dulce, in 1952 (Simon, 1969). The only event before 1960 with a reported maximum intensity (VII) as great as the main shock at Dulce was one which occurred in 1882 in the Denver-Boulder vicinity. In the mid-1960's considerable seismic activity was induced by fluid injection into the 4000 meter deep Rocky Mountain Arsenal disposal well near

Denver (Evans, 1966). Three of these events had magnitudes $m_b > 5$.

One earthquake has been reported to have affected an area very close to Dulce on May 4, 1900. According to an historical account in the Albuquerque Journal (1950), it was "a terrific earthquake shock . . . especially severe at Monero, Lumberton, and Edith." No magnitude or intensity values for this event are available.

A third reason for studying the earthquake at Dulce is its proximity to important tectonic features; the Colorado Plateau, the Rio Grande graben, and the Southern Rocky Mountains. Any information which can be learned about the seismicity of this area may contribute to an understanding of the current tectonics of these geologically and geophysically important regions and their relation to plate tectonics (Isacks et al., 1968).

A fourth reason for studying the Dulce shock is that its epicenter lies within 40 kilometers of the nuclear explosion, Gasbuggy. This underground detonation took place southwest of Dulce (36.68° north latitude, 107.21° west longitude) on December 10, 1967, at 19h 30m 00.1s GMT. The purpose of this man-made shock was to determine the feasibility of stimulating gas production with underground nuclear explosions. A fairly complete report of the seismic aspects of Gasbuggy is given by Reagor et al., (1968).

The body wave magnitude of the Gasbuggy explosion was about the same as that of the Dulce shock. The near coincidence in locations and similarity in magnitudes permits a comparative study of these two types of seismic events which is seldom possible. In addition, the accurately known origin time and coordinates of Gasbuggy provide the control necessary to accurately determine origin time and location for the Dulce earthquake.

Purpose of the Dissertation

The purpose of this dissertation is four-fold: (1) to improve the location of the Dulce shock using the nuclear explosion, Gasbuggy, as a control; (2) to determine the focal mechanism of the Dulce earthquake; (3) to compare the magnitudes of the earthquake with those of the nuclear explosion; and (4) to ascertain the fault parameters of both events from all available information.

Macroseismic Observations of the Dulce Shock

An account of macroseismic effects of the earthquake is given in U. S. Earthquakes, 1966 (Von Hake and Cloud, 1968). On the basis of interviews conducted in person and by postcard questionnaire, the earthquake was assigned a maximum intensity of VII. The isoseismal areas are roughly circular with the radii approximately as follows: VII, three kilometers; VI, seven kilometers; IV-V, fifty kilometers; I-III, 100 kilometers. However, macroseismic information to

the west of Dulce is quite sparse, owing to a very low population density. Nevertheless, as the town of Dulce was the sole victim of any significant damage, it appears likely that the epicenter was not far from the town. The factual observations which follow were made by F. H. Werner and J. P. Hoffman of U. S. Coast and Geodetic Survey's seismological observatory at Albuquerque and were taken from U. S. Earthquakes, 1966. Further details of the effects of the tremor are contained therein.

The earthquake was felt at distances of more than 100 kilometers, covering an area of about 40,000 square kilometers (15,000 square miles). The greatest damage, in Dulce, occurred at two schools: The Bureau of Indian Affairs (BIA) School and the Dulce Independent Schools. At the latter, damage included 162 broken window panes, a great deal of cracked masonry, but apparently no basic structural damage.

The BIA School complex suffered extensive interior and exterior damage. Two-story dormitories at this school, located within 1000 feet of the buildings of the Dulce Independent Schools, showed vertical cracks running from ground to roof in some of their outside walls. It is unknown to this writer whether the walls that cracked were structural members; however, these buildings were evacuated for a time subsequent to the earthquake. Another BIA building, nearly sixty years old, had bricks displaced about two

inches from vertical alignment and a sixty-foot smoke stack leaned so much that only guy wires prevented its falling.

In contrast to the relative violence of the shock at Dulce, the village of Lumberton, not more than about seven kilometers to the east, experienced only slight damage. For example, St. Francis Catholic Parish, in that community, had only minor damage to its church and school, which are constructed primarily of adobe, a construction material well-known for its vulnerability to seismic tremors. Likewise, twenty kilometers to the south of Dulce, an old adobe house suffered no damage. To the northeast about eight kilometers at Edith, Colorado, the shock was felt by all of its five or six resident families, but damage was confined to a few fallen objects.

Two rather interesting, and perhaps meaningful, observations are the reports of north-south motion of the ground, as judged by the direction in which most objects fell, and accompanying rumbling noise coming from the general direction of Archuleta Mesa (just north of Dulce), as reported by observers northeast, east, and south of Dulce.

Numerous aftershocks followed the Dulce earthquake, the largest of magnitude $m_b = 4.6$, but no foreshocks were reported. During the first week following the main shock the Albuquerque seismological center recorded 119 events from the Dulce area. Three temporary seismic stations were installed by personnel of the Albuquerque center in the

vicinity of Dulce on January 28. During the first week of their operation these stations recorded 218 aftershocks. A few of the largest aftershocks were located as shown on the map of Figure 2-6.

Geology of the Dulce Area

The town of Dulce lies in Rio Arriba County, New Mexico, at the east side of the Jicarilla Apache Indian Reservation and about eight kilometers south of the New Mexico-Colorado border.

The epicentral region of the Dulce earthquake lies near the northeast rim of the San Juan Basin where the basin joins the Archuleta Arch. This is very close to the eastern boundary of the Colorado Plateaus Province where that province joins the Southern Rocky Mountains Province.

In this area the exposed rocks consist of the following, in order of increasing age: Animas Formation, Fruitland Formation, Pictured Cliffs Sandstone, Lewis Shale, Mesaverde Formation, and Mancos Shale, all of Upper Cretaceous age.

North of the town of Dulce is Archuleta Mesa, topped by an augite-andesite sill which was intruded into the Animas Formation during Miocene time. Slightly younger than the sill on Archuleta Mesa is a swarm of north-south trending biotite-hornblende lamprophyre dikes, extending southward from the New Mexico-Colorado border over an area 60

kilometers long and about 25 kilometers wide. Still younger, but also of Miocene age, are normal faults which, in the vicinity of Dulce, strike about N30°W and are downthrown to the southwest. One such fault is clearly visible, even from some distance away, in the sill on top of Archuleta Mesa. The three features, Archuleta Mesa, the lamprophyre dikes, and the faults, are shown in Figure 2-6. Additional geologic information is available in Dane (1948) and Bingler (1968).

2. REVISION OF LOCATION AND ORIGIN TIME

Introduction

U. S. Coast and Geodetic Survey (Von Hake and Cloud, 1968) calculated the coordinates of the main Dulce earthquake to be 37.0° north latitude by 107.0° west longitude and the origin time to be 01h 56m 38.8s GMT. These values were determined by computer techniques which began with an assumed hypocenter and origin time and, through successive iterations, converged to values of these quantities which had minimum standard deviations (Engdahl and Gunst, 1966). The location corresponds to a point about 10 kilometers north of Dulce.

The nuclear explosion, Gasbuggy, was detonated within 40 kilometers of Dulce. Because of Gasbuggy's near proximity to Dulce, its well-known coordinates and origin time were used in this dissertation as a basis for revising the origin parameters of the Dulce earthquake.

Method

Basis of the Method.

The basic principles of the method developed in this paper are outlined by Richter (1958, p. 318-319). Briefly, this technique involves the following steps:

(1) Assume an approximate epicenter and origin time (TO1).

(2) Determine distances (DIST1) and azimuths (AZ1) from this epicenter to each station.

(3) Calculate the travel time (P - TO1) using the observed arrival time of P and find the corresponding distance (DIST) from the epicenter.

(4) Subtract DIST1 from DIST and call this difference the distance residual, DRES. Plot DRES for each station against the corresponding azimuth.

(5) Fit the resulting graph to a sinusoid curve whose argument variable is the azimuth, AZ1. The required adjustment in epicentral location may be read directly from this graph on the basis of the principles which follow below.

Principles of the Method.

Figure 2-1 shows a hypothetical case in which the fitted curve has the form

$$DRES = B + A \sin(AZ1 + \phi), \qquad (2\text{-}1)$$

where $A = 0.20$, $B = 0.015$ and $\phi = -45^{\circ}$. The parameter A is the distance of shift (in degrees) from the assumed epicenter, while the value of azimuth at which the curve is a maximum, in this case 135°, is the direction of the shift. At 135° DIST1 is too small and therefore the true epicenter lies farther away from stations lying in that direction by an amount equal to A.

The parameter B is a measure of the incorrectness of choice of origin time. If the origin time is chosen

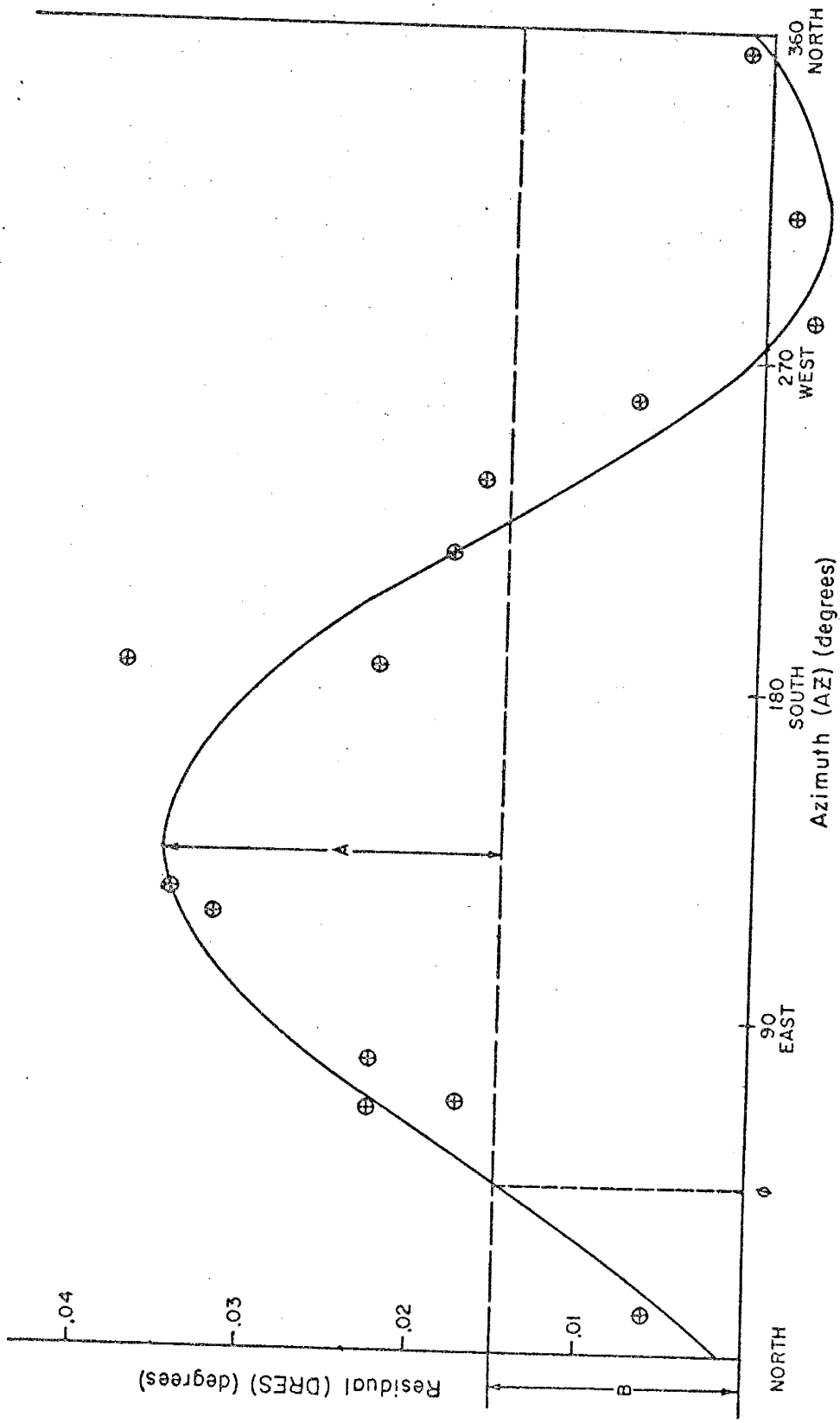

Figure 2-1. Example of plot of distance residuals as a function of azimuth.

correctly, B is zero. If, instead of calculating the distance residuals, we calculate the time residuals,

$$TRES = (P - T01)\ (obs) - (P - 0)\ (calc), \qquad (2\text{-}2)$$

where (P - 0) (calc) is based on the distance to the assumed epicenter, we would now obtain a curve of time residual as a function of azimuth. If the average time residual is too large, the "observed" values of (P - T01) are, on the average, too large. This in turn means that the quantity T01 is too small (too early), i.e., the correct value of origin time is later than the one which was assumed.

Some of the possible errors in the above procedure should be pointed out. For the most part, these are azimuthal variations of travel time about the epicenter arising from variations in crustal and upper mantle structure. This type of variation may show some symmetry as in the case when the Moho dips uniformly beneath the focus; or it may be quite randomly related to azimuth as in the case when the crustal rock is non-uniform near the focus. In addition, geologic conditions beneath the individual stations can have an effect on the travel times.

Still another source of error lies in the applicability of the travel-time tables used. Because seismic velocities vary from region to region, no single set of travel-time tables is applicable to all regions. For example, it is quite unlikely that the 1968 Seismological Tables for

P Phases (Herrin et al., 1968) used in this dissertation, apply to northern New Mexico very accurately.

Most of the errors mentioned above can be removed by adopting a procedure which involves using the differences between the corresponding residuals for Gasbuggy and the main Dulce earthquake.

Actual Method Used; Gasbuggy Control.

There are two ways in which an underground nuclear explosion can be used to improve the epicentral determination of an earthquake occurring nearby. The first method is to utilize the explosion to produce a travel-time curve or table that is uniquely applicable to that focal region and to the seismic stations involved. This procedure can remove all errors arising from variations in (1) crustal and upper mantle structure, and (2) geologic conditions near the stations. The problems associated with a standard travel-time curve (or table) are eliminated because the one produced is unique to the focal region and travel paths to which it applies.

The second method, the one used in this study, accomplishes the same result and eliminates the need for the intermediate step of assembling travel-time data into a curve or table. This technique is to plot the differences between the residuals for the two events,

$$DELR = RES(Dulce) - RES(Gasbuggy), \qquad (2\text{-}3)$$

where RES refers either to the distance residual or the time residual. The abscissa is the azimuth from the epicentral region to the seismograph station. In this study, the two events are separated by about 40 kilometers so that an average value of the azimuths with respect to the two events is used. For example, in the case of the closest station (ALQ), the difference between the two values is 10° (160° versus 170°) and the average value of 165° is therefore used in plotting ALQ's residuals. For all the 75 stations used, 10° is the greatest difference between the two azimuthal values.

Figure 2-2 is a diagram of the distance residuals for Gasbuggy, using the 1968 Seismological Tables for P Phases (Herrin et al., 1968). Even though that event's location and origin time are well known, the residuals are not small. The observed residuals indicate the 1968 Seismological Tables do not accurately give travel times from events occurring in the neighborhood of Dulce, New Mexico.

Figure 2-3 is a diagram of the distance residuals for the Dulce shock, using the same travel-time tables. The distance residuals consist of two superimposed components. The first is nearly the same set of residuals as seen in Figure 2-2 for Gasbuggy; the second is the set of residuals due to incorrect choice of epicentral coordinates and origin time for the earthquake. If the Gasbuggy residuals are subtracted from the residuals of the Dulce shock, the first

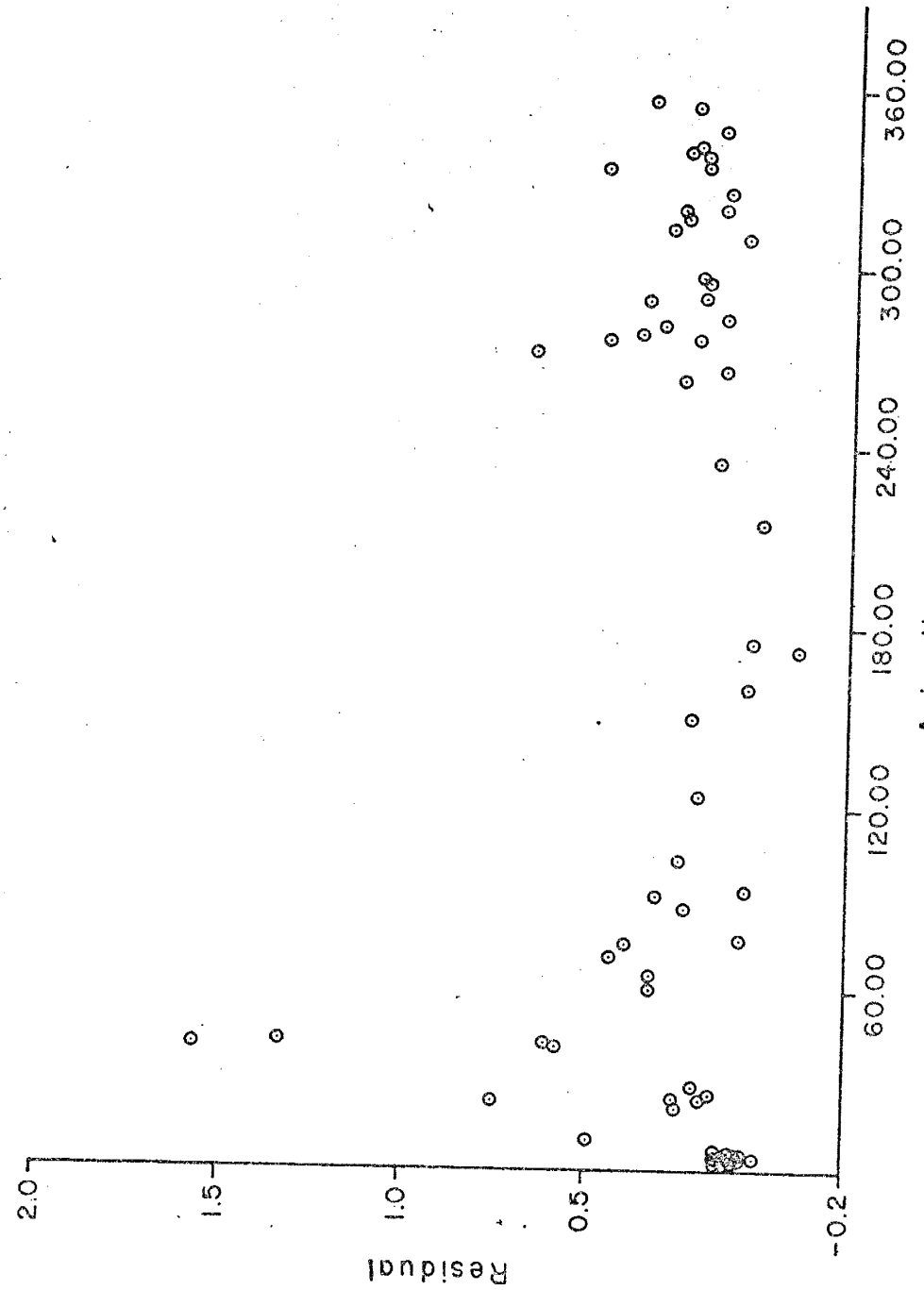

Figure 2-2. Distance residuals for Gasbuggy.

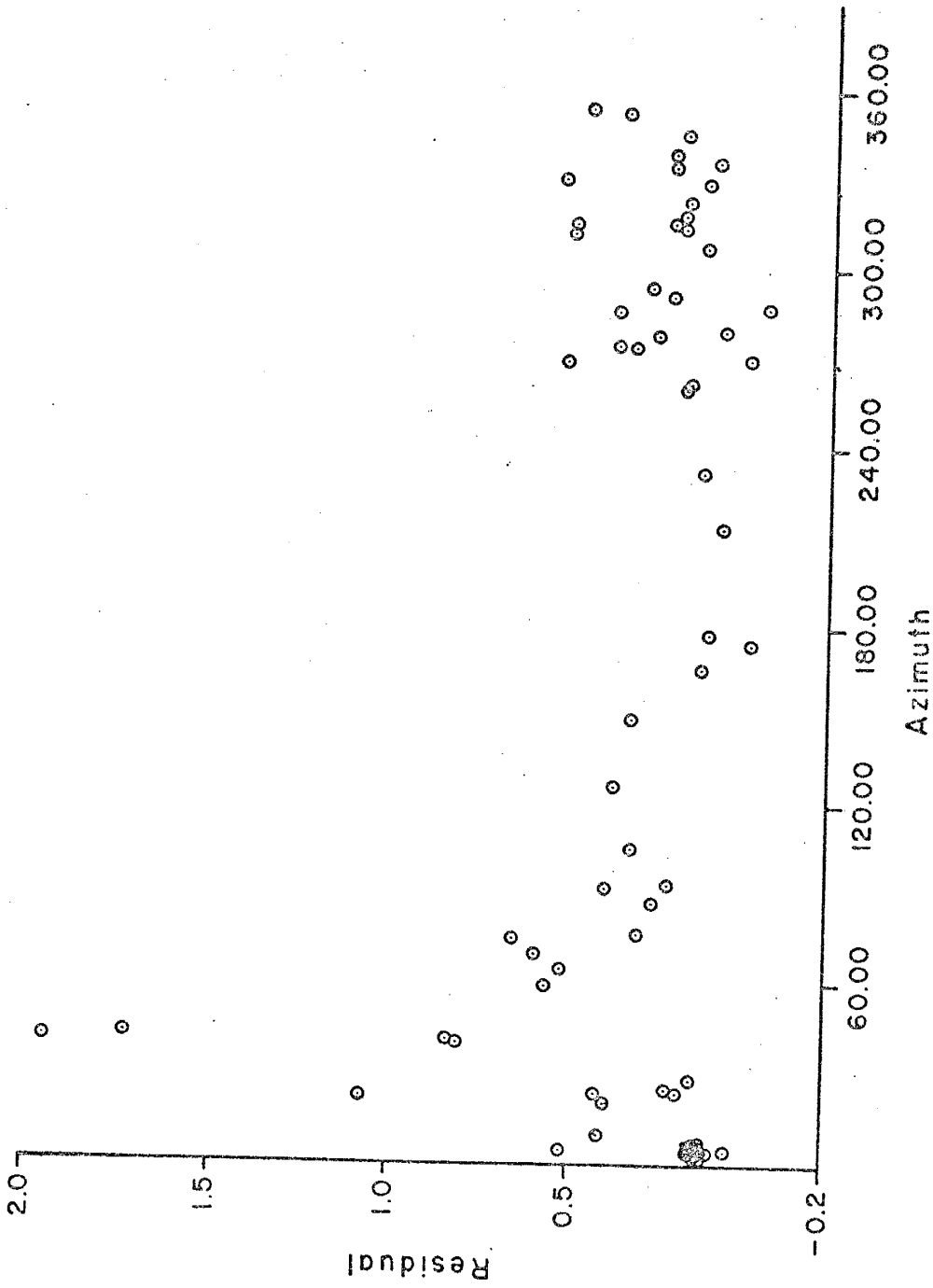

Figure 2-3. Distance residuals for the Dulce earthquake.

component is eliminated. The second component, the set of residuals which remains, yields information on the required shift in epicentral coordinates and origin time for the earthquake.

Tables 2-1A and 2-1B list the data used in constructing Figures 2-2 and 2-3, respectively. Table 2-2 gives the data used in Figures 2-4A and 2-4B which are the plots, respectively, of distance and time residual differences for the two events.

Both Figures 2-4A and 2-4B show a great deal of scatter, especially in a 90° quadrant centered along the north-south line. However, visual examination shows that a sine curve with phase $\phi = 0$ (see Equation 2-1) is a fair fit to the data. To test this possibility a least square fit was made to an equation of the form,

$$RES = A0 + A1 \sin(AZ + \phi),$$

with $\phi = 0$. The result for the data in Figure 2-4A was

$A0 = + 0.062$ deg, and

$A1 = + 0.131$ deg.

That the condition $\phi = 0$ was a correct assumption is evidenced by the fact that $A0 = 0.062$ lies within the cluster of points for the 20 LASA (Large Aperature Seismic Array) stations, which are located very nearly due north of Dulce.

In a similar manner, a least square fit of the same form was applied to the data displayed in Figure 2-4B and

Table 2-1A. Station Data Pertinent to the Epicenter Location for the Main Dulce Shock.

Station	Distance (deg)	Distance (Km)	P-Arrival (GMT) h m s	Time Residual (sec)	Distance Residual (deg)
AO	9.73	1081	01 58 59.6	1.8	0.14
B1	9.80	1089	01 59 00.4	1.7	0.12
B2	9.68	1075	01 58 58.5	1.4	0.10
B3	9.70	1078	01 58 59.0	1.6	0.12
B4	9.81	1090	01 59 00.7	1.8	0.14
C1	9.88	1098	01 59 01.9	2.0	0.15
C2	9.72	1080	01 58 59.4	1.8	0.13
C3	9.61	1068	01 58 57.8	1.5	0.11
C4	9.77	1085	01 59 00.0	1.7	0.12
D1	9.90	1100	01 59 01.6	0.8	0.06
D3	9.58	1064	01 58 57.4	1.6	0.11
D4	9.98	1109	01 59 03.0	1.8	0.13
E1	10.21	1134	01 59 06.4	2.1	0.16
E2	9.61	1068	01 58 58.0	1.9	0.14
E3	9.19	1021	01 58 52.1	1.7	0.12
E4	9.79	1088	01 59 00.2	1.6	0.12
F1	10.47	1163	01 59 10.0	2.0	0.15
F2	9.00	1000	01 58 49.6	1.8	0.13
F3	9.00	1000	01 58 49.6	1.8	0.13
F4	10.44	1160	01 59 09.3	1.9	0.14
AAM	18.61	2068	02 01 00.0	6.0	0.52
ALQ	2.06	229	01 57 14.6	1.9	0.14

Table 2-1A. (continued)

Station	Distance (deg)	Distance (Km)	P-Arrival (GMT) h m s	Time Residual (sec)	Distance Residual (deg)
BCN	6.45	717	01 58 15.3	2.4	0.18
BMO	11.11	1234	01 59 20.7	2.7	0.20
BOU	3.29	366	01 57 32.8	2.8	0.20
BOZ	9.33	1037	01 58 55.4	3.1	0.23
BUT	9.98	1109	01 59 02.7	1.5	0.11
CMC	31.20	3466	02 03 00.0	3.2	0.36
COL	36.79	4087	02 03 49.9	4.5	0.53
CPO	17.22	1913	02 00 40.5	3.4	0.27
DEN	3.18	353	01 57 30.4	2.2	0.16
DUG	5.63	625	01 58 04.1	2.1	0.15
EDM	16.86	1873	02 00 35.0	2.5	0.20
EPT	5.21	579	01 57 56.0	0.2	0.01
EUR	7.55	839	01 58 31.3	3.2	0.23
FGU	4.40	489	01 57 47.2	3.1	0.23
FLN	72.31	8034	02 08 07.9	4.7	0.80
GCA	3.75	417	01 57 36.6	0.6	0.02
GOL	2.98	331	01 57 28.5	3.0	0.22
GRR	72.36	8039	02 08 08.7	4.9	0.82
GSC	8.17	908	01 58 39.0	2.6	0.19
HCU	3.69	410	01 57 38.0	2.8	0.20
JAS	10.78	1198	01 59 15.6	3.7	0.27
KTG	53.82	5979	02 06 03.2	3.1	0.42
LOG	6.09	677	01 58 10.6	2.6	0.19

Table 2-1A. (continued)

Station	Distance (deg)	Distance (Km)	P-Arrival (GMT) h m s	Time Residual (sec)	Distance Residual (deg)
LON	14.75	1639	02 00 12.0	6.7	0.50
LOR	74.64	8293	02 08 26.9	9.9	1.70
LUB	5.33	592	01 58 02.6	5.1	0.38
MAT	85.20	9466	02 09 16.5	2.5	0.50
MBC	39.66	4406	02 04 13.2	3.8	0.46
MHC	11.74	1304	01 59 29.9	5.1	0.38
NOR	53.52	5946	02 06 01.0	3.0	0.41
NRR	10.48	1164	01 59 07.6	-0.4	-0.03
NUR	74.37	8263	02 08 21.6	6.2	1.06
ORV	11.74	1304	01 59 30.0	5.1	0.38
OTT	24.75	2750	02 02 04.0	5.3	0.56
OXF	14.39	1599	02 00 03.6	3.1	0.23
PBJ	22.92	2546	02 01 44.1	3.3	0.33
PRI	11.08	1231	01 59 23.0	7.0	0.52
RCD	7.63	848	01 58 34.6	5.3	0.39
RES	38.14	4237	02 04 01.0	4.3	0.51
SCP	22.82	2535	02 01 45.8	5.8	0.59
SLC	5.40	600	01 58 01.7	3.1	0.23
SLD	11.42	1269	01 59 25.1	4.5	0.33
SLM	13.25	1472	01 59 49.5	4.1	0.31
SNM	2.90	322	01 57 25.8	1.6	0.12
SSF	74.33	8258	02 08 26.4	11.2	1.92
TFO	4.45	494	01 57 47.3	1.9	0.14

Table 2-1A. (continued)

Station	Distance (deg)	Distance (Km)	P-Arrival (GMT) h m s	Time Residual (sec)	Distance Residual (deg)
TNP	8.25	917	01 58 38.8	1.2	0.09
TUC	5.65	628	01 58 03.2	1.3	0.09
TUL	8.99	999	01 58 53.0	5.4	0.40
UBO	3.94	438	01 57 40.8	1.9	0.14
UNV	9.44	1049	01 58 57.7	4.0	0.29
WMO	7.10	789	01 58 26.4	4.5	0.33
WSC	23.45	2605	02 01 52.6	6.4	0.65

Table 2-1B. Station Data Pertinent to the Epicenter Location for Gasbuggy.

Station	Distance (deg)	Distance (Km)	P-Arrival (GMT) h m s	Time Residual (sec)	Distance Residual (deg)
A0	10.04	1115	19 32 26.0	1.2	0.08
B1	10.11	1123	19 32 26.9	1.1	0.08
B2	9.99	1110	19 32 25.0	0.9	0.06
B3	10.00	1111	19 32 25.5	1.2	0.09
B4	10.11	1123	19 32 27.2	1.3	0.11
C1	10.19	1132	19 32 27.7	0.8	0.06
C2	10.03	1114	19 32 25.5	0.8	0.06
C3	9.92	1102	19 32 24.3	1.1	0.08
C4	10.08	1120	19 32 26.3	1.0	0.07
D1	10.21	1134	19 32 28.4	0.6	0.03
D3	9.89	1099	19 32 24.0	1.3	0.09
D4	10.28	1142	19 32 29.9	1.8	0.13
E1	10.52	1169	19 32 32.7	1.4	0.10
E2	9.93	1103	19 32 24.5	1.2	0.08
E3	9.49	1054	19 32 18.9	1.5	0.11
E4	10.09	1121	19 32 26.7	1.2	0.10
F1	10.80	1200	19 32 36.9	1.8	0.13
F2	9.32	1035	19 32 16.4	1.3	0.10
F3	9.30	1033	19 32 16.1	1.4	0.10
F4	10.74	1193	19 32 35.8	1.5	0.11
AAM	18.96	2106	19 34 25.0	3.7	0.32
ALQ	1.84	204	19 30 33.4	1.0	0.07

Table 2-1B. (continued)

Station	Distance (deg)	Distance (Km)	P-Arrival (GMT) h m s	Time Residual (sec)	Distance Residual (deg)
BCN	6.18	687	19 31 34.3	2.0	0.15
BMO	11.17	1241	19 32 43.9	3.7	0.27
BOU	3.66	407	19 31 00.1	2.4	0.18
BOZ	9.52	1058	19 32 20.9	3.1	0.23
BUT	10.16	1129	19 32 29.4	2.9	0.21
CMC	31.47	3496	19 36 24.7	2.1	0.24
COL	36.94	4104	19 37 13.8	4.1	0.48
CPO	17.48	1942	19 34 06.4	2.9	0.23
DEN	3.55	394	19 30 58.9	2.7	0.20
DUG	5.62	624	19 31 26.0	1.4	0.10
EDM	17.09	1899	19 34 00.7	2.1	0.17
EPT	4.94	549	19 31 14.5	-0.8	-0.06
EUR	7.44	827	19 31 52.2	2.7	0.20
FGU	4.58	509	19 31 12.7	3.5	0.26
FLN	72.69	8076	19 41 32.6	3.4	0.57
GCA	3.52	391	19 30 58.8	3.0	0.22
GOL	3.35	372	19 30 55.6	2.1	0.15
GRR	72.75	8083	19 41 33.1	3.6	0.60
GSC	7.88	875	19 31 59.0	3.5	0.26
HCU	3.74	416	19 31 01.0	2.2	0.16
JAS	10.59	1177	19 32 36.7	4.4	0.32
KTG	54.19	6021	19 39 28.2	1.8	0.25
LOG	6.19	688	19 31 34.2	2.0	0.15

Table 2-1B. (continued)

Station	Distance (deg)	Distance (Km)	P-Arrival (GMT) h m s	Time Residual (sec)	Distance Residual (deg)
LON	14.80	1644	19 33 37.6	8.7	0.66
LOR	75.03	8336	19 41 50.5	7.6	1.32
LUB	5.35	594	19 31 23.6	2.7	0.20
MAT	85.22	9468	19 42 39.3	1.5	0.30
MBC	39.94	4437	19 37 38.3	3.0	0.36
MHC	11.53	1281	19 32 50.3	5.2	0.38
NOR	53.86	5984	19 39 27.5	3.5	0.48
NRR	10.35	1150	19 32 32.0	2.9	0.21
NUR	74.74	8304	19 41 45.5	4.3	0.74
ORV	11.59	1288	19 32 50.7	4.9	0.36
OTT	25.11	2790	19 35 28.5	3.0	0.32
OXF	14.61	1623	19 33 27.3	0.9	0.07
PBJ	22.78	2531	19 35 05.2	2.2	0.22
PRI	10.83	1203	19 32 44.5	8.9	0.66
RCD	8.00	889	19 32 00.3	3.2	0.24
RES	38.46	4273	19 37 24.0	1.1	0.13
SCP	23.14	2571	19 35 10.8	4.2	0.43
SLC	5.46	607	19 31 42.6	2.2	0.16
SLD	11.21	1245	19 32 47.4	6.4	0.47
SLM	13.56	1507	19 33 13.5	1.1	0.08
SNM	2.62	291	19 30 44.0	0.8	0.06
SSF	74.72	8301	19 41 50.1	9.0	1.55
TFO	4.08	453	19 31 05.7	2.2	0.16

Table 2-1B. (continued)

Station	Distance (deg)	Distance (Km)	P-Arrival (GMT) h m s	Time Residual (sec)	Distance Residual (deg)
TNP	8.07	897	19 32 00.1	2.1	0.15
TUC	5.27	585	19 31 20.4	0.6	0.04
TUL	9.23	1025	19 32 18.0	4.2	0.31
UBO	4.09	454	19 31 06.4	2.9	0.21
UNV	9.35	1039	19 32 18.3	3.0	0.22
WMO	7.27	808	19 31 50.5	3.4	0.25
WSC	23.76	2640	19 35 16.5	3.8	0.39

Table 2-2. Residual Differences (Dulce - Gasbuggy)

Station	Average Azimuth (deg CW from N)	Time Residual Difference (Dulce - Gasbuggy) (sec)	Distance Residual Difference (Dulce - Gasbuggy) (deg)
** AO	3	0.6	0.04
** B1	3	0.6	0.04
** B2	3	0.5	0.04
** B3	2	0.4	0.03
** B4	3	0.5	0.04
** C1	3	1.2	0.09
** C2	4	1.0	0.07
** C3	3	0.4	0.03
** C4	2	0.7	0.05
** D1	4	0.2	0.01
** D3	2	0.3	0.02
** D4	2	0.0	0.00
** E1	3	0.7	0.05
** E2	6	0.7	0.05
** E3	2	0.2	0.01
** E4	0	0.4	0.03
** F1	6	0.2	0.01
** F2	6	0.5	0.04
** F3	359	0.4	0.03
** F4	0	0.4	0.03
AAM	66	2.3	0.19
**ALQ	165	0.9	0.06

Table 2-2. (continued)

Station	Average Azimuth	Time Residual Difference (sec)	Distance Residual Difference (deg)
**BCN	265	0.4	0.03
BMO	319	-1.0	-0.07
**BOU	23	0.4	0.03
**BOZ	340	0.0	0.00
BUT	337	-1.4	-0.10
CMC	354	1.1	0.12
COL	332	0.4	0.05
CPO	87	0.5	0.04
DEN	27	-0.5	-0.04
**DUG	308	0.7	0.05
EDM	347	0.4	0.03
EPT	175	1.0	0.07
**EUR	293	0.5	0.04
**FGU	337	-0.4	-0.03
FLN	42	1.3	0.23
GCA	273	-2.4	-0.18
**GOL	24	0.9	0.07
GRR	42	1.3	0.22
**GSC	262	-0.9	-0.07
HCU	317	0.6	0.04
JAS	280	-0.7	-0.05
KTG	25	1.3	0.17
LOG	324	0.6	0.04

Table 2-2. (continued)

Station	Average Azimuth	Time Residual Difference (sec)	Distance Residual Difference (deg)
LON	316	-2.0	-0.15
LOR	41	2.3	0.38
LUB	126	2.4	0.18
MAT	313	1.0	0.20
MBC	355	0.8	0.10
MHC	277	-0.1	-0.01
NOR	11	-0.5	-0.07
NRR	289	-3.3	-0.24
NUR	23	1.9	0.32
ORV	288	0.2	0.02
OTT	60	2.3	0.24
OXF	94	2.2	0.17
PBJ	151	1.1	0.11
PRI	270	-1.9	-0.14
RCD	20	2.1	0.15
RES	5	3.2	0.38
SCP	71	1.6	0.16
SLC	318	0.9	0.07
SLD	275	-1.9	-0.14
SLM	78	3.0	0.22
**SNM	178	0.8	0.06
SSF	41	2.2	0.37
**TFO	234	-0.3	-0.02

Table 2-2. (continued)

Station	Average Azimuth	Time Residual Difference (sec)	Distance Residual Difference (deg)
TNP	282	-0.9	-0.07
**TUC	216	0.7	0.05
TUL	92	1.2	0.09
**UBO	331	-1.0	-0.07
UNV	296	1.0	0.07
**WMO	105	1.1	0.08
WSC	76	2.6	0.26

** These stations were used in the final determination of the epicenter of the Dulce earthquake.

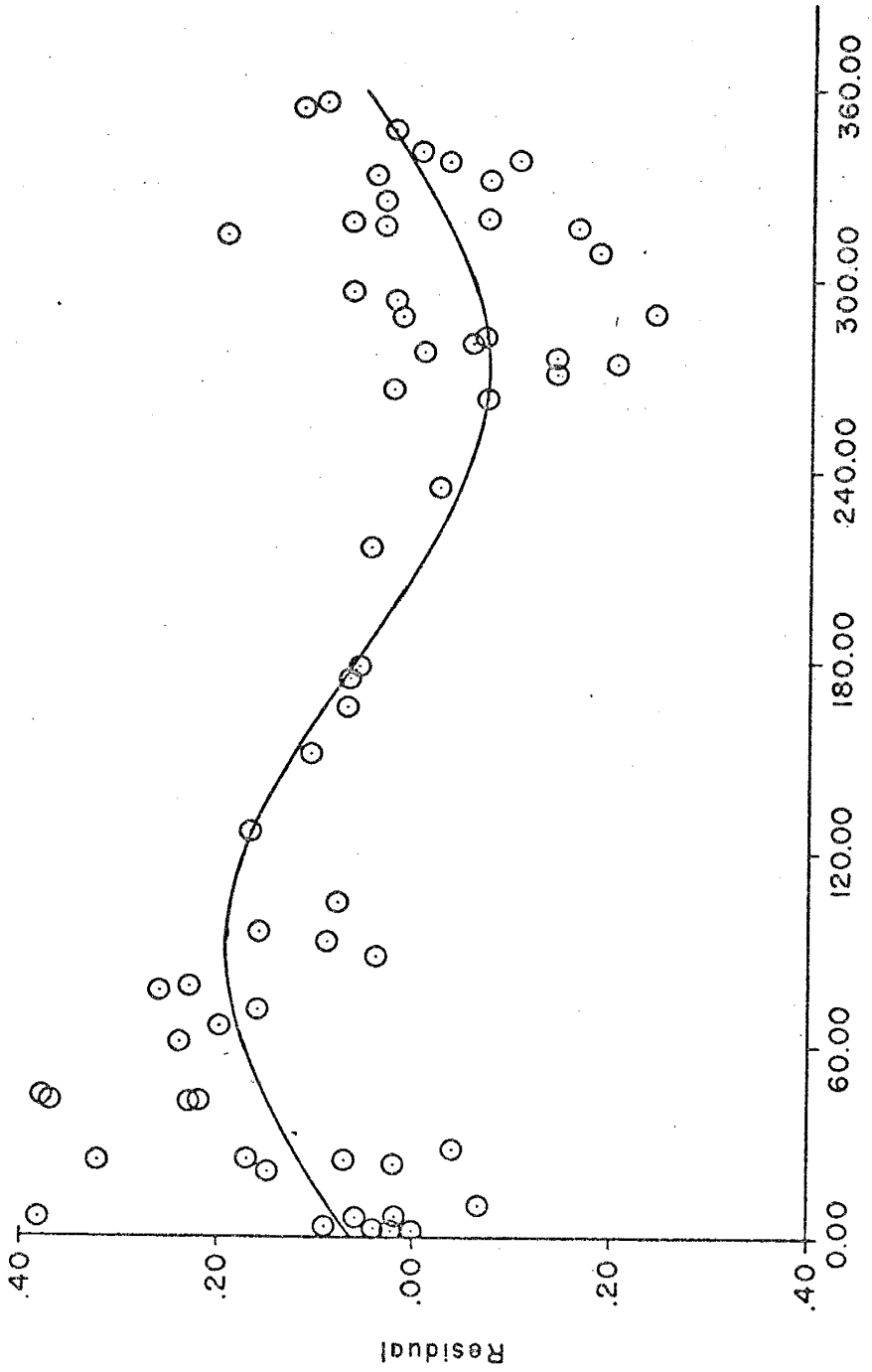

Figure 2-4A. Difference in distance residuals between Gasbuggy and the Dulce earthquake.

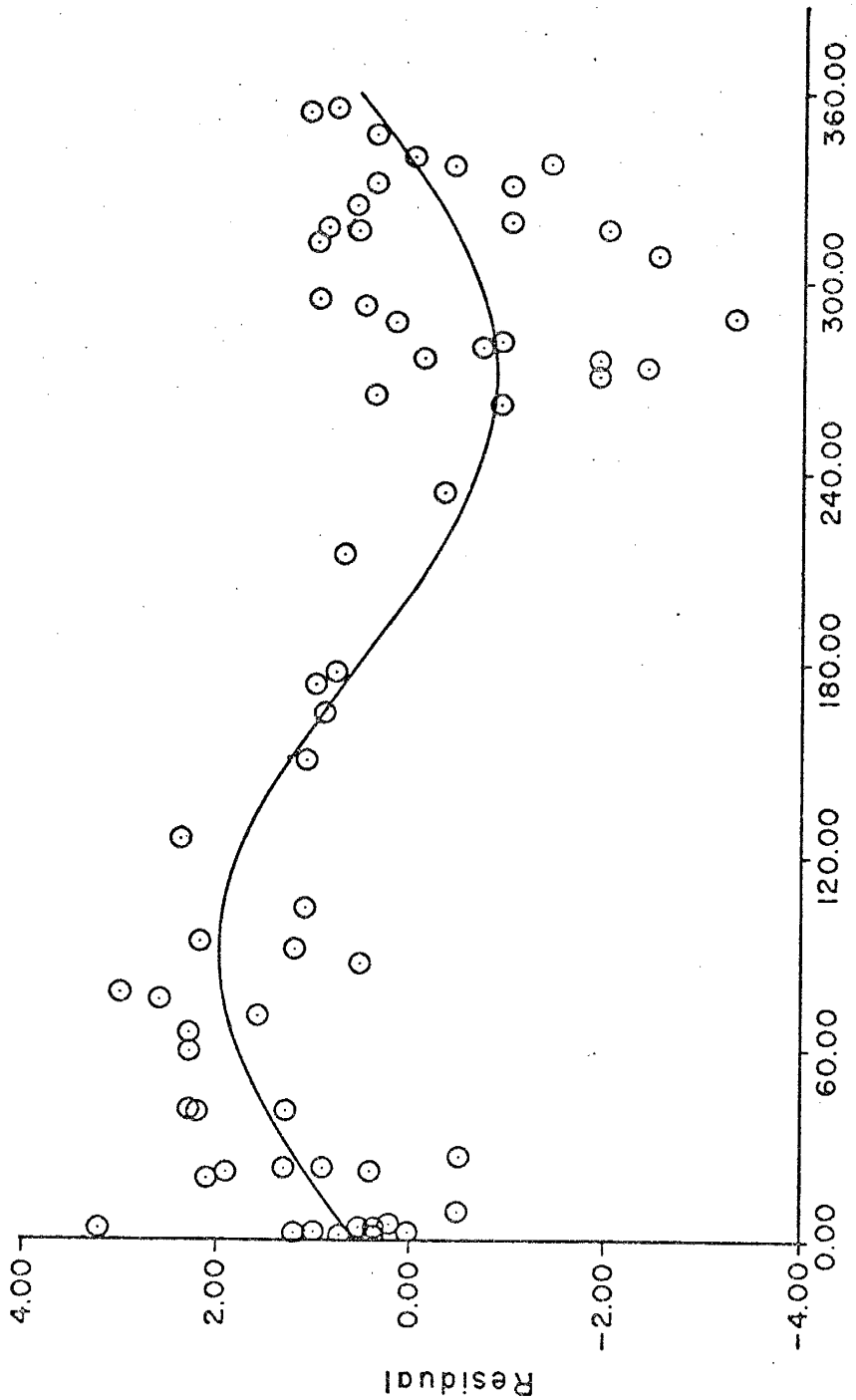

Figure 2-4B. Difference in time residuals between Gasbuggy and the Dulce earthquake.

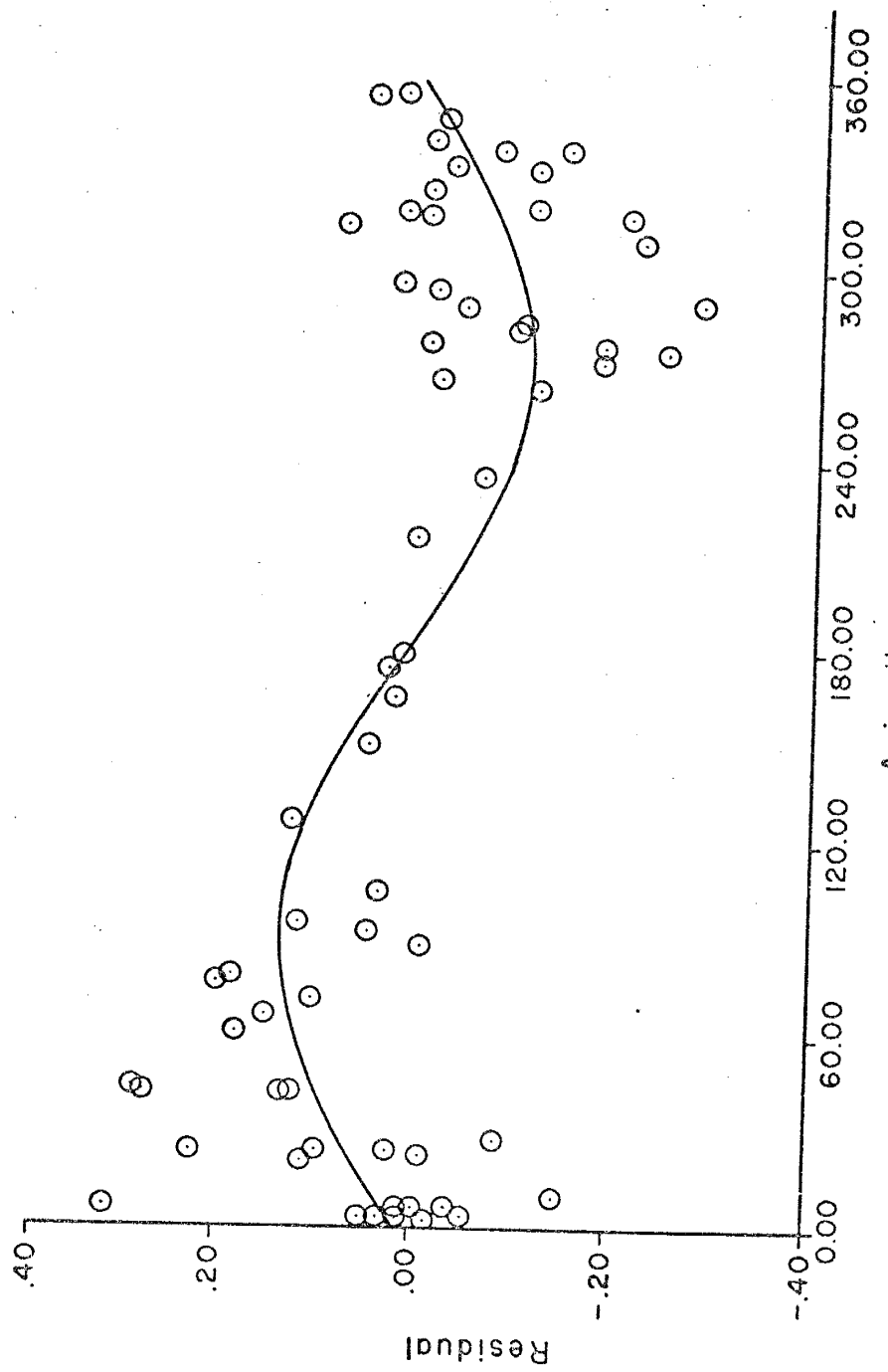

Figure 2-4C. Adjusted difference in distance residuals between Gasbuggy and the Dulce earthquake.

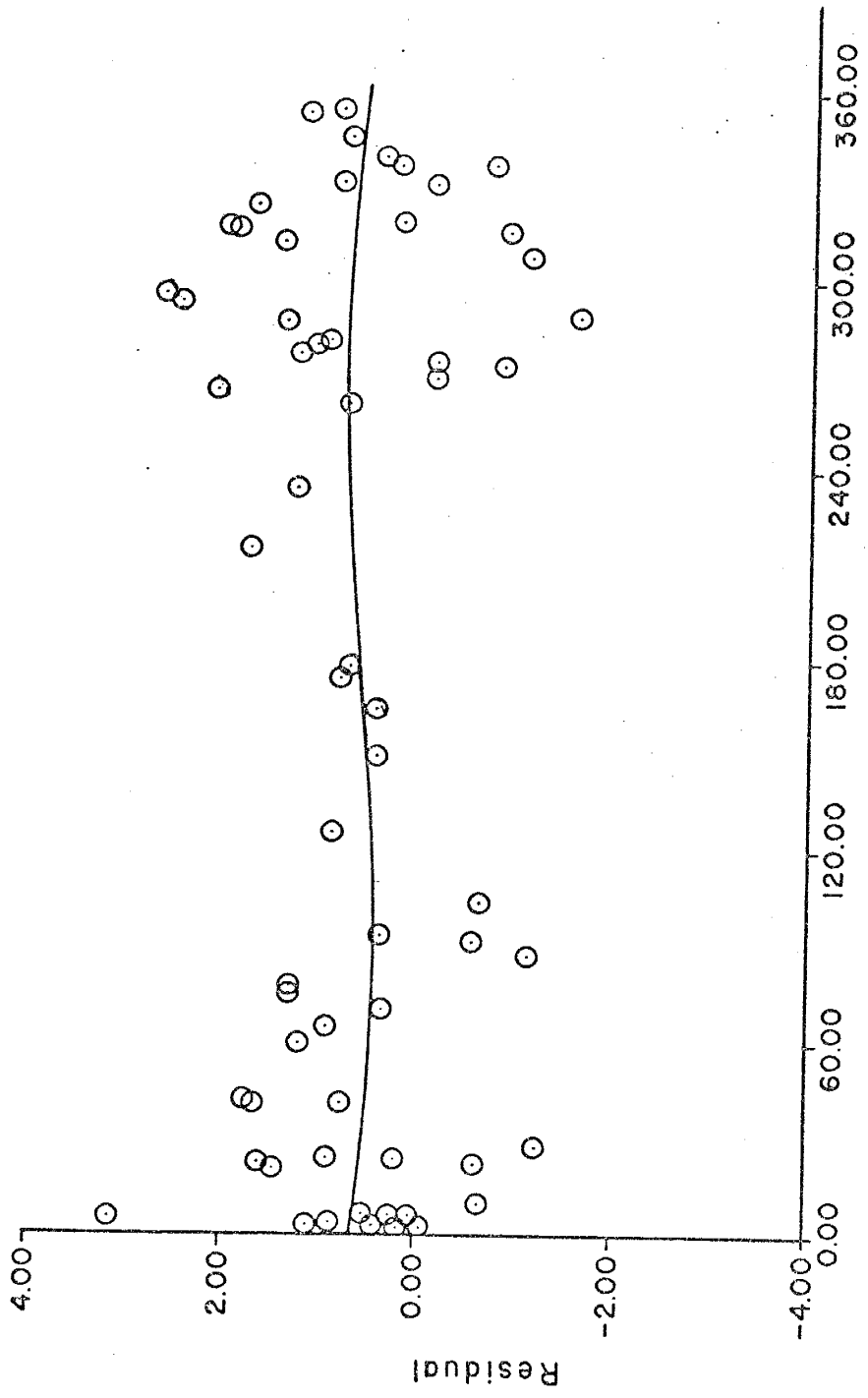

Figure 2-4D. Adjusted difference in time residuals between Gasbuggy and the Dulce earthquake.

the parameters,

A0 = + 0.555 sec, and

A1 = + 1.428 sec,

were obtained.

In order to see the residuals due to origin time and those due to epicenter separately, Figures 2-4C and 2-4D were constructed. Figure 2-4C displays the distance residual curve after the effects of origin time error are removed. Figure 2-4D exhibits the time residual curve after the sinusoidal distance residuals are eliminated.

Results

Adjustment of the Epicenter.

From Figure 2-4C, the least square fit yields parameters,

A0 = + 0.014 deg, and

A1 = + 0.122 deg, with a computed

SD = 0.105 deg (standard deviation).

Ideally, of course, A0 should be zero. The value obtained, however, amounts to only about one kilometer, well within the standard deviation.

The parameter A1 indicates that the epicenter should be moved about 0.12° along a great circle to the west. This corresponds to 0.15° longitude at a latitude of 37° and to a distance of 13.3 kilometers. Figure 2-6, a map of the area, shows the assumed epicenter (39.96°N, 107.05°W), as

well as the aftershocks located by Werner and Hoffman (unpublished report) (triangles) and by U. S. Coast and Geodetic Survey (circles).

Because of the large standard deviation, the seismograms were re-examined and only those with sharp initial onsets chosen for a re-run of the above procedure. These stations are marked with a double asterisk (**) in Table 2-2 and the residual plots are shown in Figures 2-5A through 2-5D.

In Figure 2-5C,

AO = + 0.002 deg,

A1 = + 0.044 deg, and the computed

SD = 0.044 deg.

This result is considerably different from the determination that used data from all stations. The epicenter is adjusted to the west by 0.044° of a great circle which corresponds to 0.055° longitude or 4.9 kilometers. This would establish the epicenter at 36.96°N, 106.95°W. In this case, the standard deviation is considerably smaller. The epicenter using the best arrivals is shown on the map in Figure 2-6.

Adjustment of the Origin Time.

For the time residuals in Figure 2-4D, the least square fit to a sine curve is very nearly a straight horizontal line with parameters,

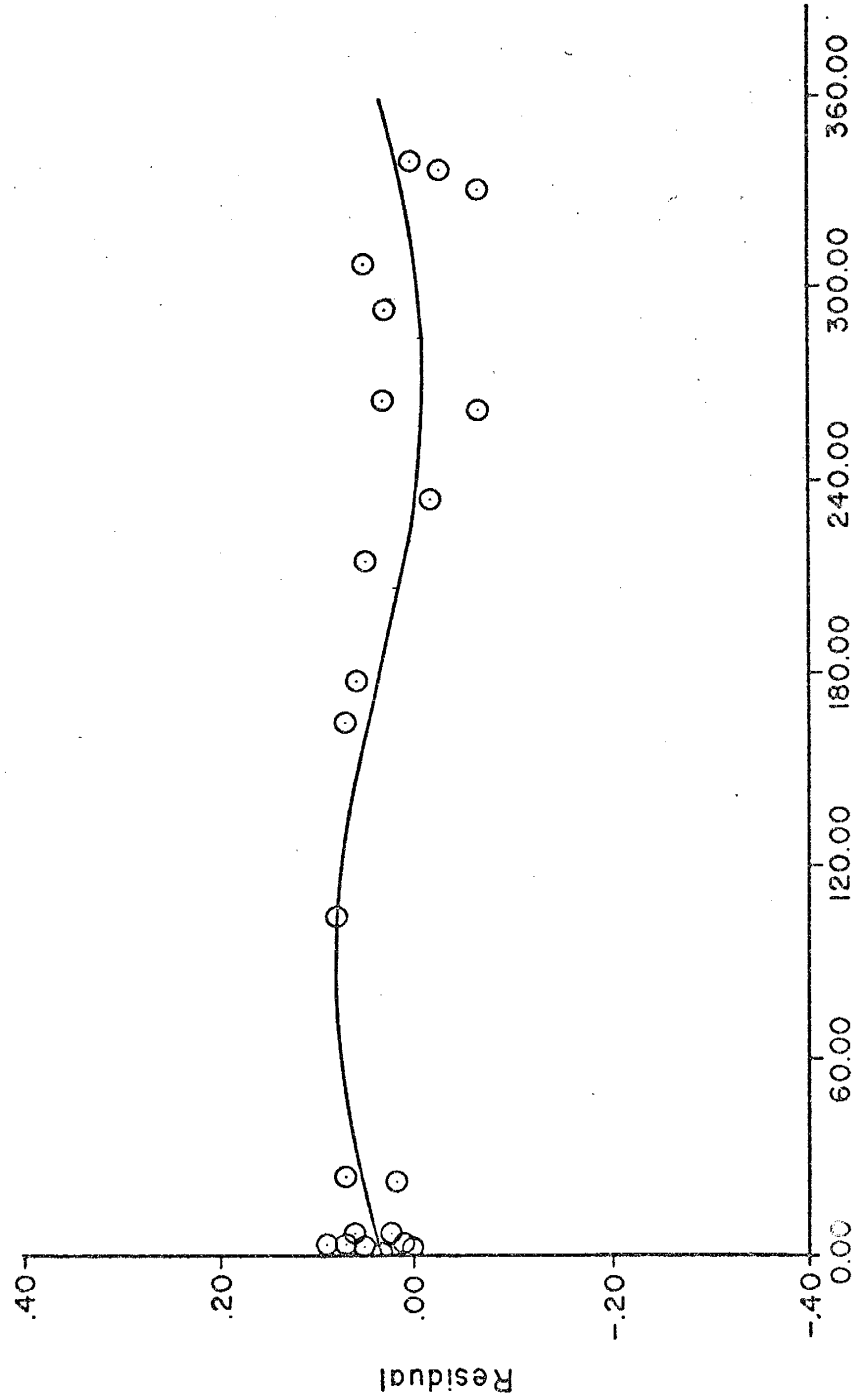

Figure 2-5A. Difference in distance residuals between Gasbuggy and the Dulce earthquake for the best stations.

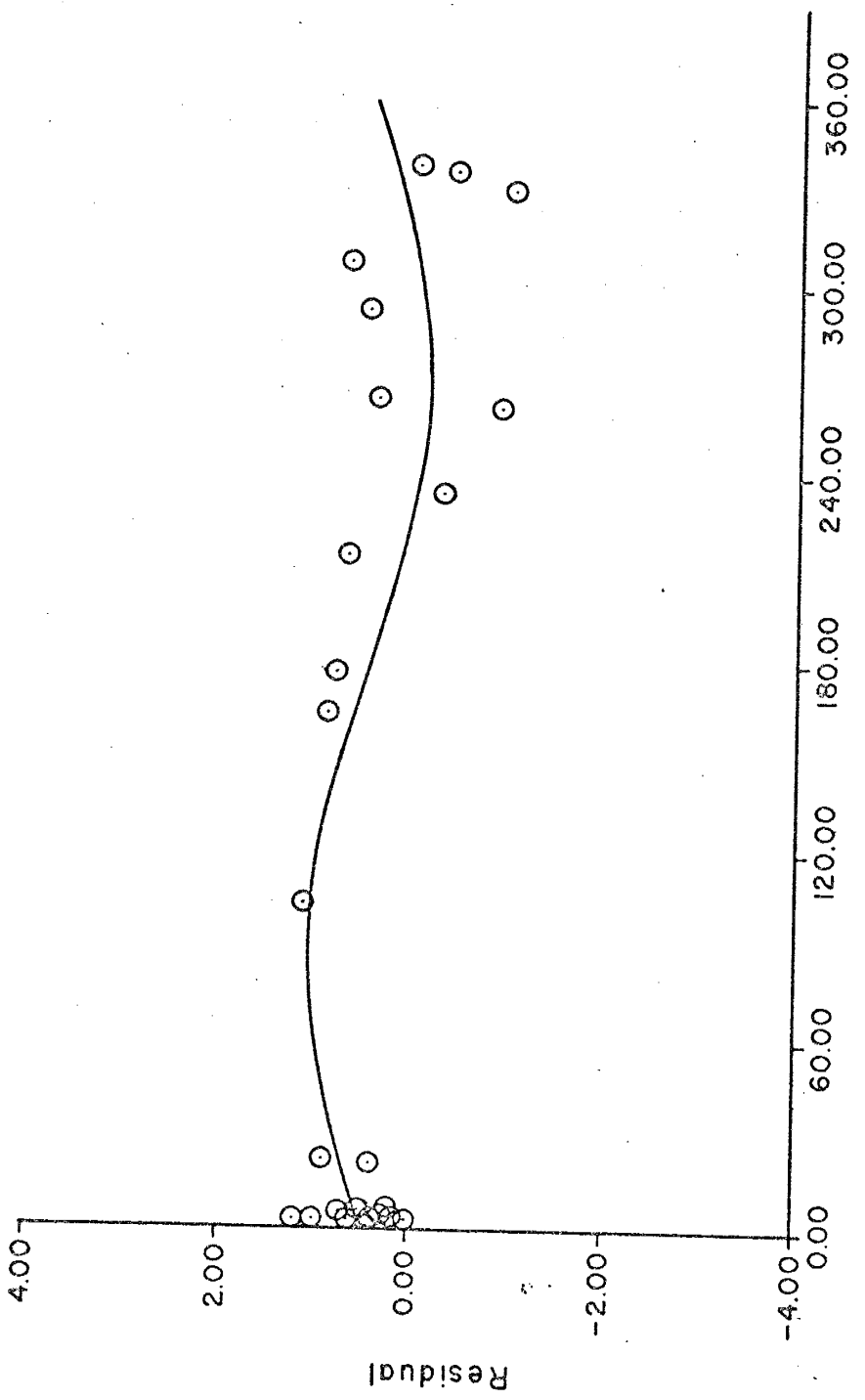

Figure 2-5B. Difference in time residuals between Gasbuggy and the Dulce earthquake for the best stations.

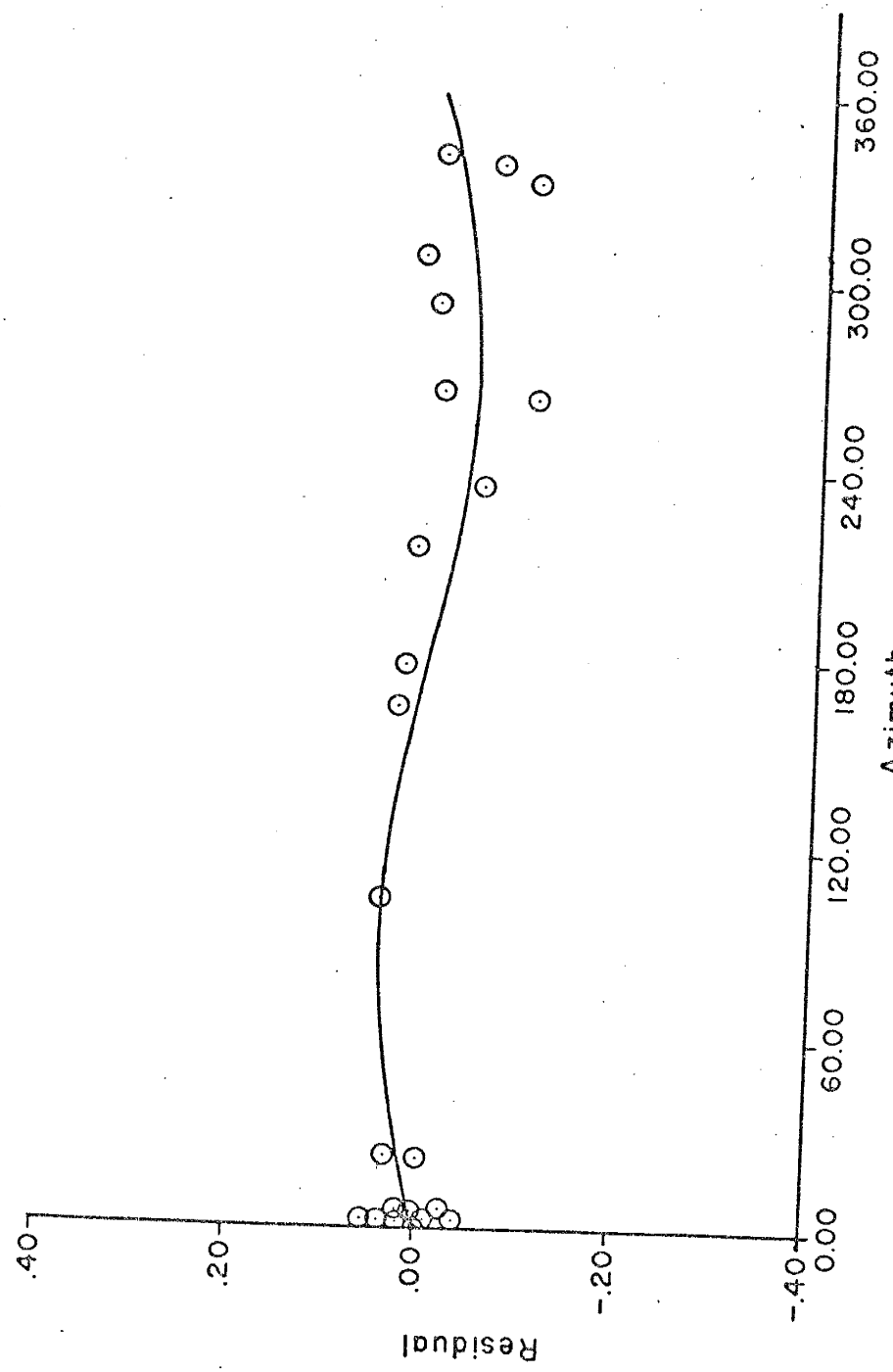

Figure 2-5C. Adjusted difference in distance residuals between Gasbuggy and the Dulce earthquake for the best stations.

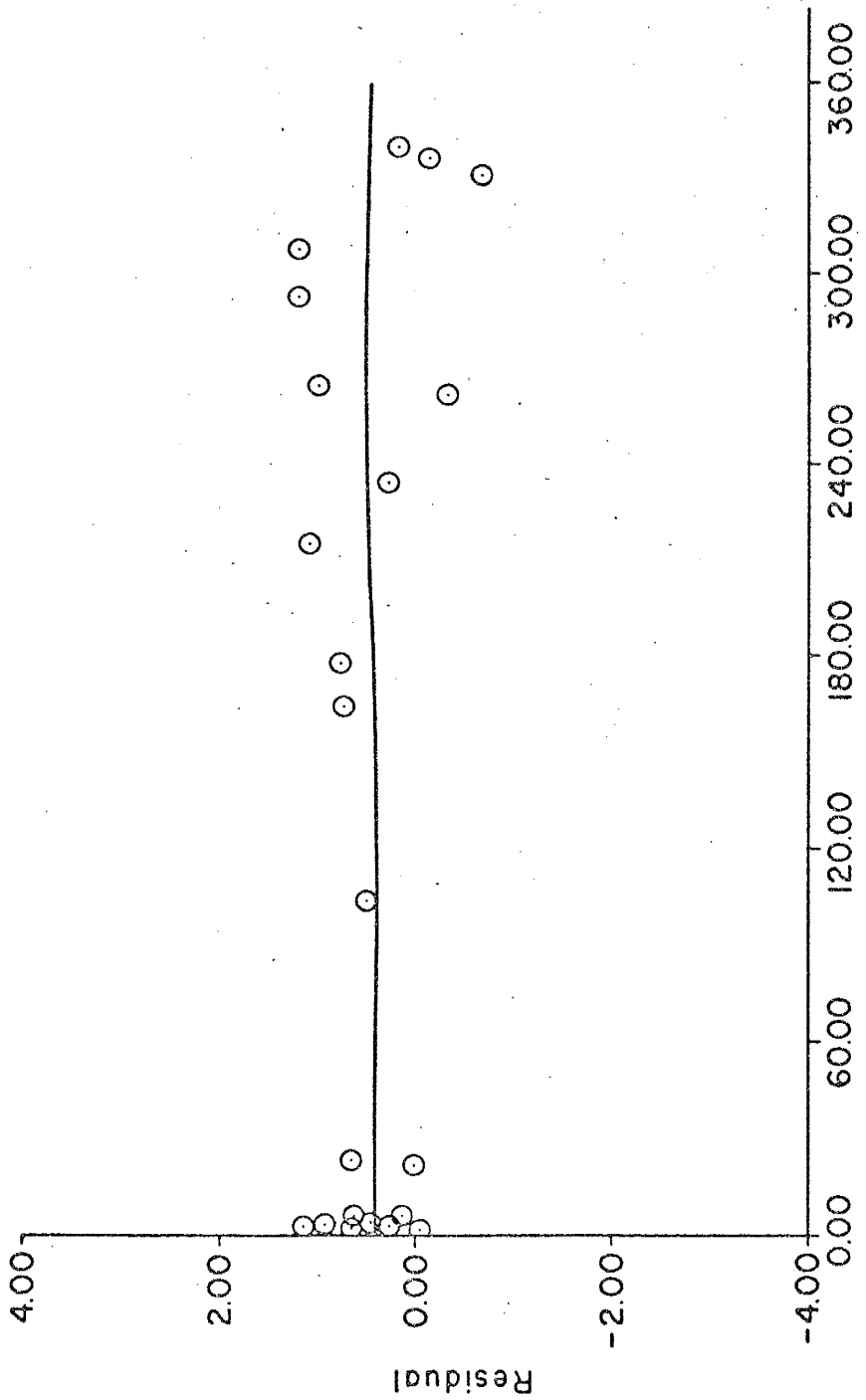

Figure 2-5D. Adjusted difference in time residuals between Gasbuggy and the Dulce earthquake for the best stations.

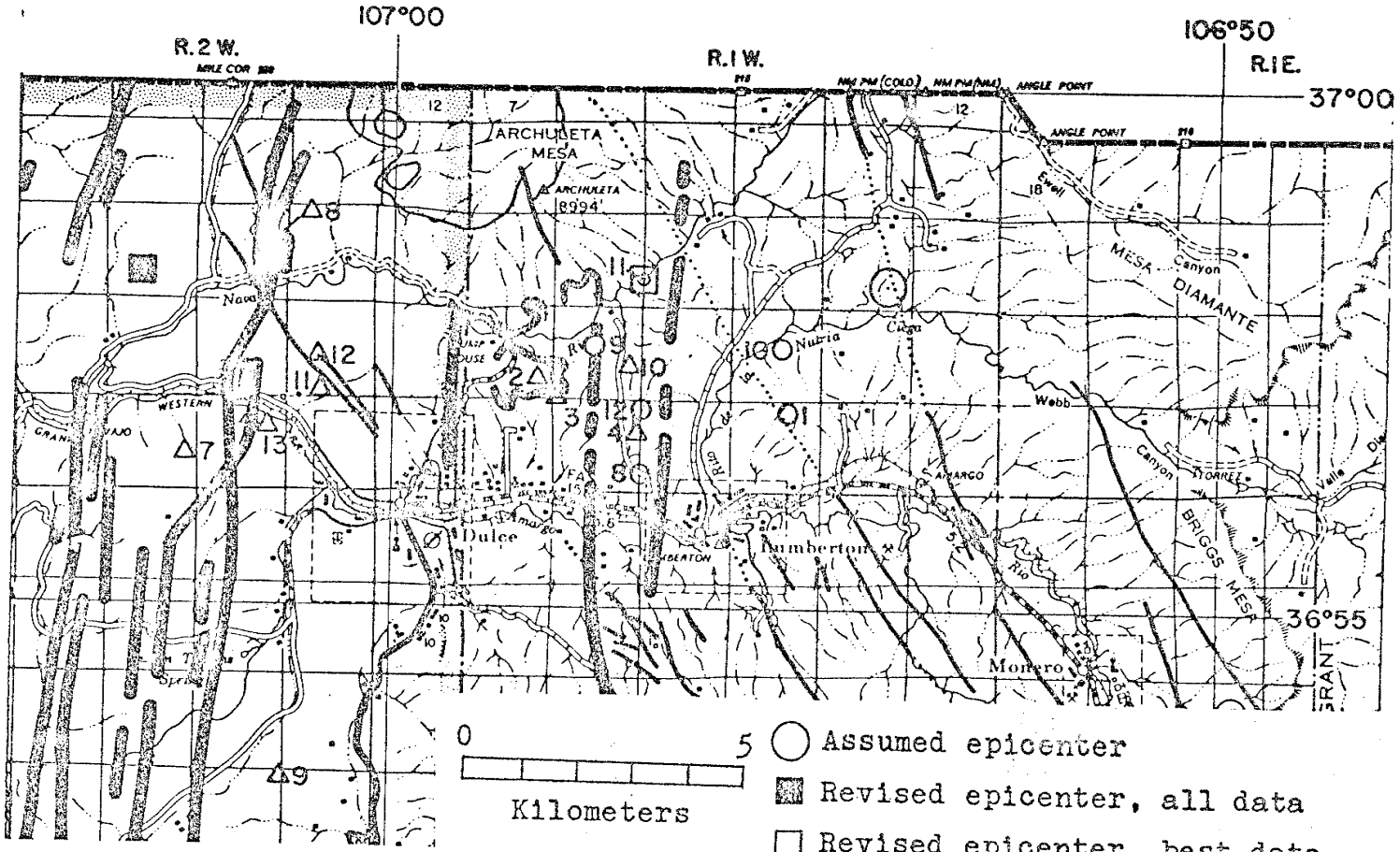

Figure 2-6. Map of the Dulce area showing the location of the main earthquake and several of the largest aftershocks and the most important geological features of the area (from Bingler, 1968).

A0 = + 0.616 sec,

A1 = - 0.181 sec, and a computed

SD = 0.917.

The result indicates the true origin time should be 0.6 second later than the assumed origin time (01h 56m 38.8s), or 01h 56m 39.4s GMT.

Figure 2-5D shows the time residuals when only the best arrivals are used. In this case, the least-square fit is not much different than that obtained by all stations, because

A0 = + 0.456 sec, and

A1 = - 0.048.

However, the computed standard deviation, 0.422 second, is considerably smaller. The time adjustment of about 0.5 second yields an origin time of 01h 56m 39.3s GMT.

Discussion of the Results.

Table 2-3 summarizes the locations and origin times obtained from using all arrival times, and from using only the best arrival times. Geologically, either of the two locations is feasible. The first, at 107.05° west longitude, is situated near the intersection of a series of north-south trending lamprophyre dikes with a northwest-southeast striking fault (Figure 2-6). This epicenter is also close to the westernmost group of aftershocks located by Werner and Hoffman (unpublished report). The second location, at 106.95 west longitude, is situated between two well-defined

Table 2-3. Summary of Results for Origin Time and Epicenter Coordinates.

	All Stations	Best Stations
Date	January 23, 1966	January 23, 1966
Time (GMT)	01h 56m 39.4s	01h 56m 39.3s
Latitude	36.96° N	36.96° N
Longitude	107.05° W	106.95° W

lamprophyre dikes, and is nearer to the highly faulted region southeast of Dulce (Figure 2-6). In addition, this epicenter is very close to the earliest aftershocks (triangles #2, 3, and 4, Figure 2-6) located by Werner and Hoffman.

3. FOCAL MECHANISM

Introduction and Purpose

The purpose of this chapter is to use the direction of the first motion of P wave arrivals at a number of seismograph stations to determine the nature of the fault mechanism that produced the Dulce earthquake.

General Review of the Nature of Faulting

The assumed mechanical model of an earthquake used in the focal mechanism study is based on the "elastic rebound" theory originated by H. F. Reid in the first decade of this century following the 1906 San Francisco earthquake. In this model, shear stress is built up in the earth's crust, due to tectonic forces, until a shear stress is reached that is sufficient to overcome friction on a pre-existing fracture or to initiate a new fracture in the earth's crust or upper mantle. The fracturing process is accompanied by sudden movement of the crust in the neighborhood of the fracture in such a direction as to relieve the tectonic stress. Rapid movement along a fracture, or fault, releases stored elastic strain energy which is in the form of longitudinal (P) and transverse (S) waves. P waves travel at about 1.73 times the speed of S waves and are therefore the first to reach any observation point.

The fault is a roughly planar fracture zone and, in principle, may have any spatial orientation. This orientation is represented by the strike and dip of the fault surface. The motion of the walls of the fault is along the fault and normal to a plane which is called the auxiliary plane. The direction and amount of the fault motion is referred to as the net slip.

Faults can be classified in several ways, depending on the orientation of the fault plane and direction of net slip. Three special cases are diagrammed in Figure 3-1:

(1) strike-slip, in which the fault plane is vertical and the motion is horizontal

(2) normal, in which the fault dips steeply and the motion is along the dip, with the "hanging wall" or upper wall moving downward

(3) thrust, in which the dip of the fault plane is at a low angle, with the hanging wall moving up-dip.

Faults observed in the field are generally complex, so the above descriptions are only good approximations. The focal mechanism solution is an attempt to determine, or at least estimate, the three parameters of a fault, the strike, dip, and direction of net slip.

Focal Mechanism from P Waves

Method.

If the directions of the first motions of P waves generated by faulting are determined at a number stations around

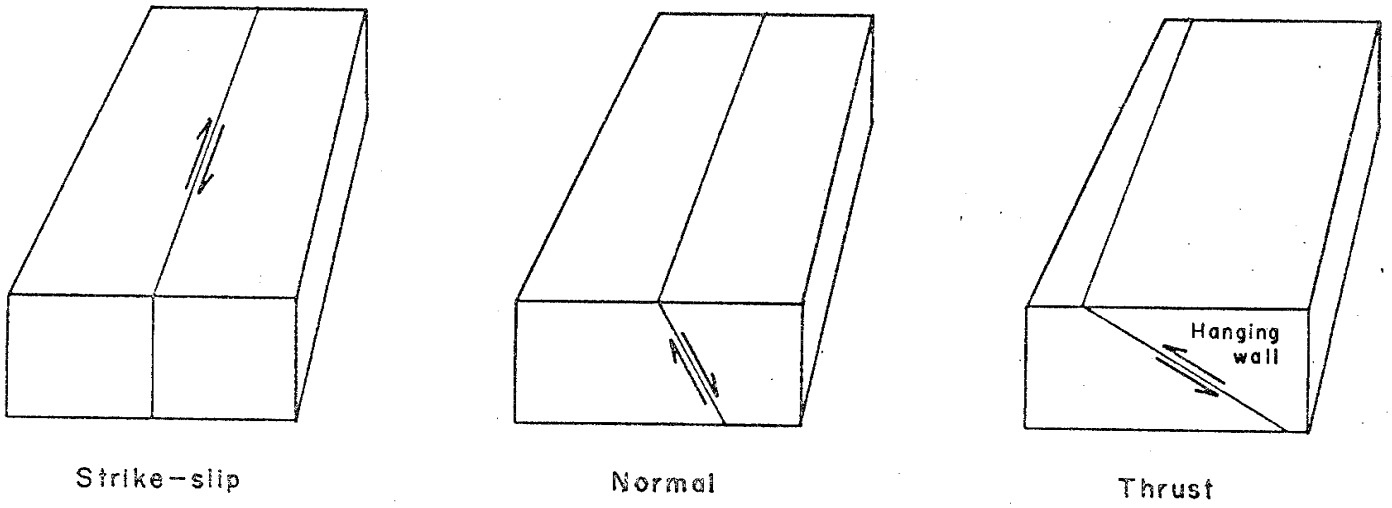

Figure 3-1. Block diagrams of three special classes of faults.

the epicenter, information about the direction and orientation of the net slip can be obtained. Figure 3-2 has been constructed so as to show the fault plane perpendicular to the page and the net slip in the plane of the page. The fault plane is represented by the dark line; the dashed line A - A' is the auxiliary plane which is normal to the direction of the net slip. The motions on either side of the fault are represented by the pair of arrows. The motion shown has a clockwise sense; if the plane of the paper were the surface of the earth, this would be referred to as a right-lateral strike-slip fault. Similarly, a strike-slip fault with a motion in the counter-clockwise sense would be called left-lateral.

If the nodal planes (fault plane and auxiliary plane) are extended indefinitely, they will segment the earth into four quadrants, which are alternately marked (+) and (-) in the figure. Theory shows that the P waves produce compressive initial motions at points in the regions marked (+) and dilatational (or rarefactional) initial motions at points in the regions marked (-). At a given seismic station on the earth's surface, the P waves arrive from below, and therefore a vertical component seismograph will record a compressive pulse as an UP ground motion and a dilatational pulse as a DOWN ground motion. This is one method of studying the fault motion; i.e., plotting first motions of P at various seismograph locations to determine the P wave radiation pattern and, from that, the probable focal mechanism.

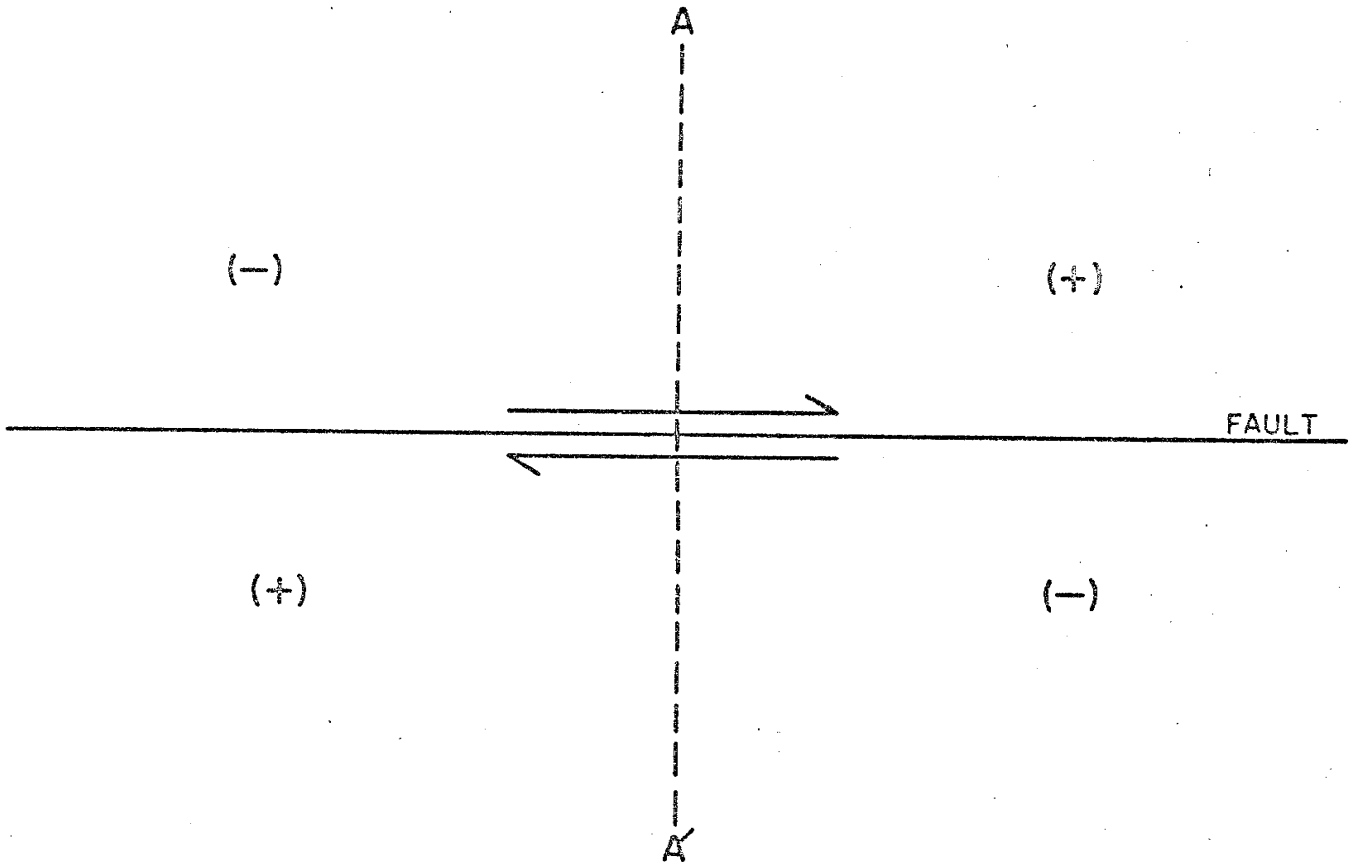

Figure 3-2. Diagram of a vertical, right-lateral, strike-slip fault showing regions of compressional (+) and dilatational (-) P wave radiation. The plane of the paper represents the horizontal plane.

This method is not without ambiguity. The P wave distribution pattern shown in Figure 3-2 could also have been obtained by interchanging the fault and auxiliary planes and drawing the vectors representing relative motion in the counter-clockwise sense.

Fault mechanisms could be determined easily by the technique described above if every earthquake originated on a strike-slip fault and the radiation pattern on the earth's surface were thus symmetrical about the epicenter as in Figure 3-2. However, as this seldom is the case, further refinements of the technique have necessarily been developed.

The technique used here employs the concept of the focal sphere and the stereographic projection, or Wulff net, commonly used in structural geology. A complete explanation of this projection can be found in Ramsay (1967, p. 1-8). The focal sphere is an imaginary sphere which encloses the focus of the earthquake, small enough so that rays from the focus pass through the focal sphere at the same angle at which they leave the source. This focal sphere is used as the unit sphere of the stereographic projection. (See, for example, Stauder, 1962, p. 13-14.)

Rays arriving at a seismograph originally left the source (and the focal sphere) at some angle, $\underline{i}$, with the vertical. The formula used for calculating $\underline{i}$ was taken from Stauder (1962):

$$\sin \underline{i} = (V_h) \cdot (R_o / R_h) \cdot (dT/d\Delta), \qquad (3\text{-}1)$$

where V_h is the P wave velocity at the focus, R_h the distance from the center of the earth to the focus, R_o the radius of the earth, and $dT/d\Delta$ the inverse of the apparent velocity of the P wave at the earth's surface. The last quantity is also the inverse of the horizontal velocity of the P wave at the deepest point on its travel path, which for Pn (the refracted P wave) is the velocity of the P wave at the top of the mantle. The factor $dT/d\Delta$ was obtained from the 1968 Seismological Tables for P Phases (Herrin et al., 1968) assuming a 15 kilometer depth of focus.

When $\underline{i}$ has been determined, the position of the seismograph station on the Wulff net is the projection of the point where the ray emerged from the focal sphere. This point is labelled as either a compression or a dilatation according to whether the seismograph recorded an UP or a DOWN first motion, respectively. The plotting of the station position is illustrated in Figure 3-3. Seismic wave velocities generally increase with increasing depth. Consequently, these rays are refracted upward and thus, for all but the closest stations (those within about 150 kilometers for shallow focus events), the recorded ray left the focus traveling downward. Since the nearest seismograph (ALQ) to the Dulce earthquake was at a distance 230 kilometers, all stations are plotted as projections of points on the lower focal hemisphere.

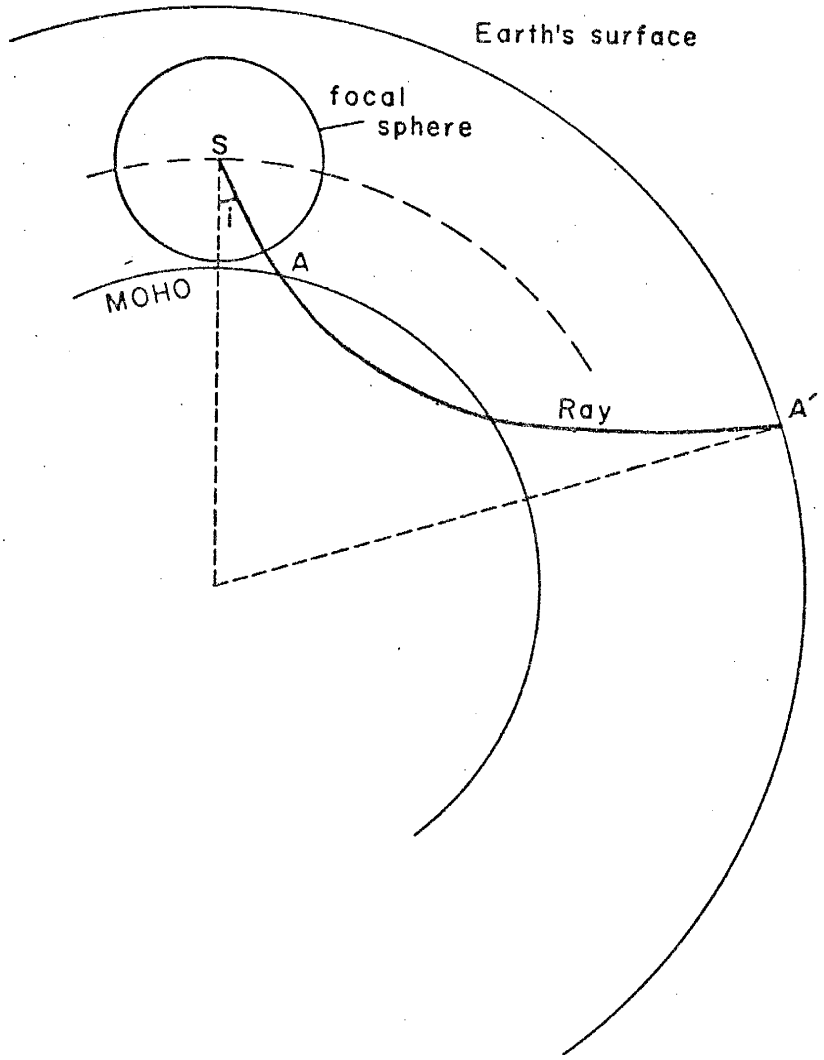

Figure 3-3. Vertical plane containing a seismic ray between the source, S, and a seismic station, A'. The ray leaves the focal sphere at point A in a downward direction and is refracted upward to the seismic station. The first motion data for that seismograph is plotted on the stereographic projection at a point corresponding to A on the focal sphere, at the azimuth of the station.

Figure 3-4 shows the manner in which the stereographic projection would be divided for three common classes of earthquakes: (1) right-lateral strike-slip, (2) normal, and (3) thrust faulting. The dark region corresponds to compressional first arrivals, the lighter regions to dilatational first arrivals. One great circle, marked F, corresponds to the stereographic projection of the fault plane; the other to the projection of the auxiliary plane.

Data and Mechanism Diagrams.

The number of stations having good first motions was not large. This is undoubtedly due to the relatively small size of the event (although Sykes (1967) and others have had some success in working with earthquakes of similar magnitude). Nevertheless, by first looking at all the available first motions, then examining the data from only the more certain first motions, and finally considering the geology of the Dulce area, a fairly certain conclusion regarding the mechanism of the event is obtained.

Table 3-1 is a listing of all the available first motion data. Most of the directions of first motion were assigned by the writer on the basis of an examination of the short-period seismograms. A few, however, were obtained from other sources, such as station bulletins, either because the records were not available or the interpretation was so uncertain that it was felt that first motions assigned by seismograph station personnel would probably be more reliable.

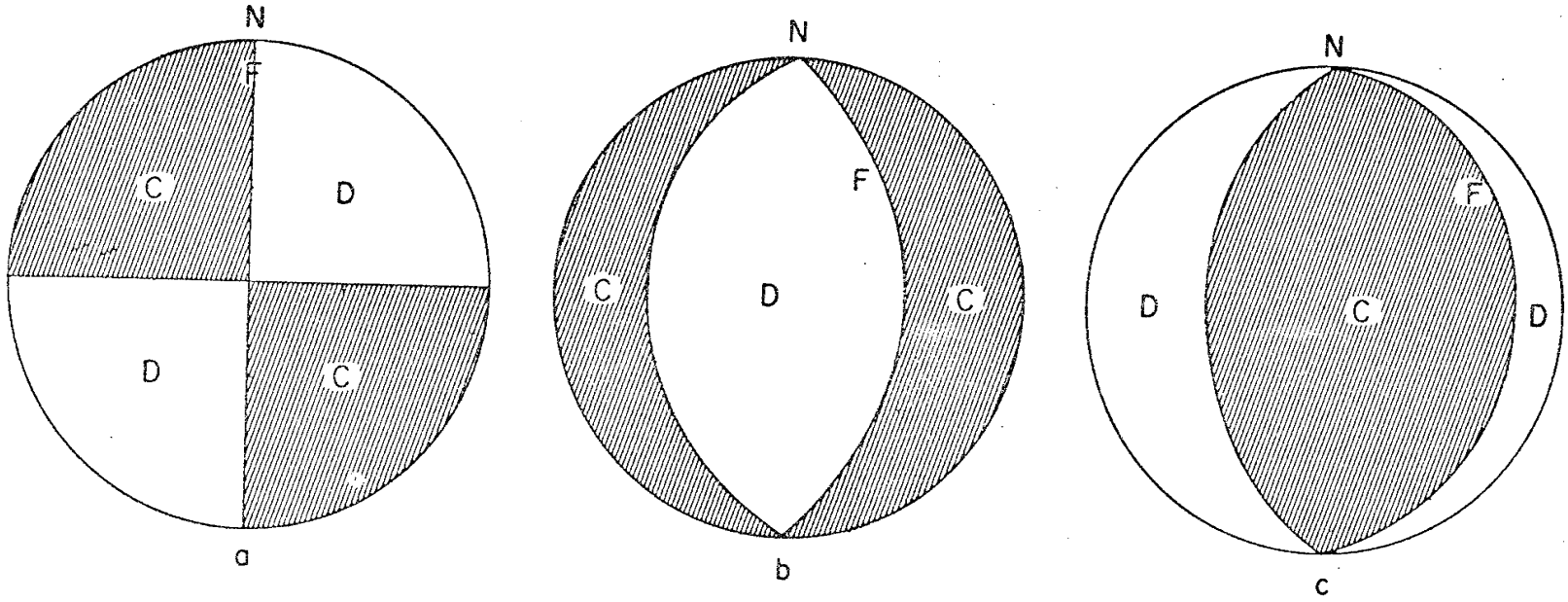

Figure 3-4. Sample mechanism diagrams. In each case, the fault strikes N-S and is marked F. (a) strike-slip, right-lateral, fault vertical, motion horizontal; (b) normal, fault dipping east, motion along dip; (c) thrust, fault dipping east, motion along dip.

Table 3-1. Listing of All Available P Wave First Motion Data.

Station	Distance (degrees)	Azimuth	i	P First Motion	Quality
AO	9.74	3	47.4	D	VG
B1	9.81	4	47.4	D	VG
B2	9.68	4	47.4	D	VG
B3	9.70	3	47.4	D	VG
B4	9.81	3	47.4	D	VG
C1	9.89	4	47.4	D	VG
C2	9.73	4	47.4	D	VG
C3	9.62	3	47.4	D	VG
C4	9.78	3	47.4	D	VG
D1	9.90	5	47.4	D	VG
D3	9.59	2	47.4	D	P
D4	9.98	3	47.4	D	VG
E1	10.22	4	47.4	D	P
E2	9.62	7	47.4	D	F
E3	9.19	3	47.4	D	VG
E4	9.79	1	47.4	D	VG
F2	9.01	7	47.4	D	VG
F3	9.00	0	47.4	D	VG
F4	10.44	0	47.4	D	VG
AAM	18.72	66	39.7	C	VP
ALQ	2.09	167	47.8	D	VG
ATL	18.85	94	39.7	D	P
BCN	6.34	263	47.8	C	F

Table 3-1. (continued)

Station	Distance (degrees)	Azimuth	i	P First Motion	Quality
BKS	12.08	279	46.9	C	*
BLA	21.17	81	35.4	D	P
BOU	3.34	24	47.8	D	P
BOZ	9.29	340	47.4	C	VG
CGM	13.95	83	46.5	D	VP
CMC	31.19	354	28.4	C	P
COL	36.74	332	28.4	C	G
DAL	9.37	113	47.4	C	P
DEN	3.23	29	47.8	D	F
DUG	5.54	307	47.8	D	P
ENM	13.29	84	46.4	D	G
EPT	5.22	175	47.8	C	P
EUR	7.44	292	47.8	C	VG
FGU	4.35	336	47.8	C	P
FLO	13.27	77	46.5	C	P
GCA	3.63	271	47.8	C	P
GOL	3.03	25	47.8	D	VG
GSC	8.05	261	47.4	C	VG
HHM	12.47	338	46.9	C	F
JAS	10.66	279	47.4	C	G
JCT	8.85	135	47.4	C	G
LON	14.67	316	45.6	C	G
LRA	12.10	96	46.9	D	F
LUB	5.42	127	47.8	D	VP

Table 3-1. (continued)

Station	Distance (degrees)	Azimuth	i	P First Motion	Quality
MDS	14.64	59	45.6	D	VP
MHC	11.62	276	46.9	D	*
MIN	11.84	291	46.9	D	*
OXF	14.51	94	45.6	D	P
PAS	9.46	256	47.4	C	VP
PBJ	22.97	150	32.8	C	VP
PRI	10.96	270	47.4	C	P
RCD	7.68	21	47.4	D	F
RGS	8.98	17	47.4	D	P
SCP	22.93	71	32.8	C	F
SLM	13.37	78	46.5	D	F
SNM	2.91	178	47.8	C	F
SWM	12.77	346	46.5	C	P
TFO	4.36	233	47.8	C	F
TNP	8.14	281	47.4	C	VG
TUC	5.58	214	47.8	D	VG
UBO	3.88	330	47.8	D	F
WMO	7.22	106	47.8	C	G
WNS	8.48	37	47.4	C	F

* Assigned by seismograph station personnel.

Figure 3-5 is the plot of data of Table 3-1 on the sterographic projection. The positions of the stations are plotted at a distance from the center of the projection corresponding to the angle of incidence at which the ray leaves the focal sphere. For most of the stations plotted, the first arrival is Pn, a compressional head wave (or conical wave) generated at the Moho (crust-mantle interface). The ray path for the Pn phase intercepts the Moho discontinuity at the critical angle. The assumption in the available seismological tables is that the Pn phase is a first arrival over large regions. Consequently, all seismographs receiving Pn as the first arrival are plotted at the same distance from the center of the projection. In this paper, no seismograph was close enough to the epicenter to receive the direct P wave through the crust as the first arrival, and therefore no station is plotted at angles of incidence greater than the critical angle (about 48^{o}). A few stations, however, are far enough from the epicenter so that the direct P wave through the mantle is the earliest signal to arrive. These stations, which are located in the eastern U. S., Alaska, and southern Mexico, have smaller angles of incidence and therefore are plotted closer to the center of the Wulff net.

Most of the important features of the distributions of compressions and dilatations are apparent in Figure 3-5. One of the most convincing aspects of the diagram is the

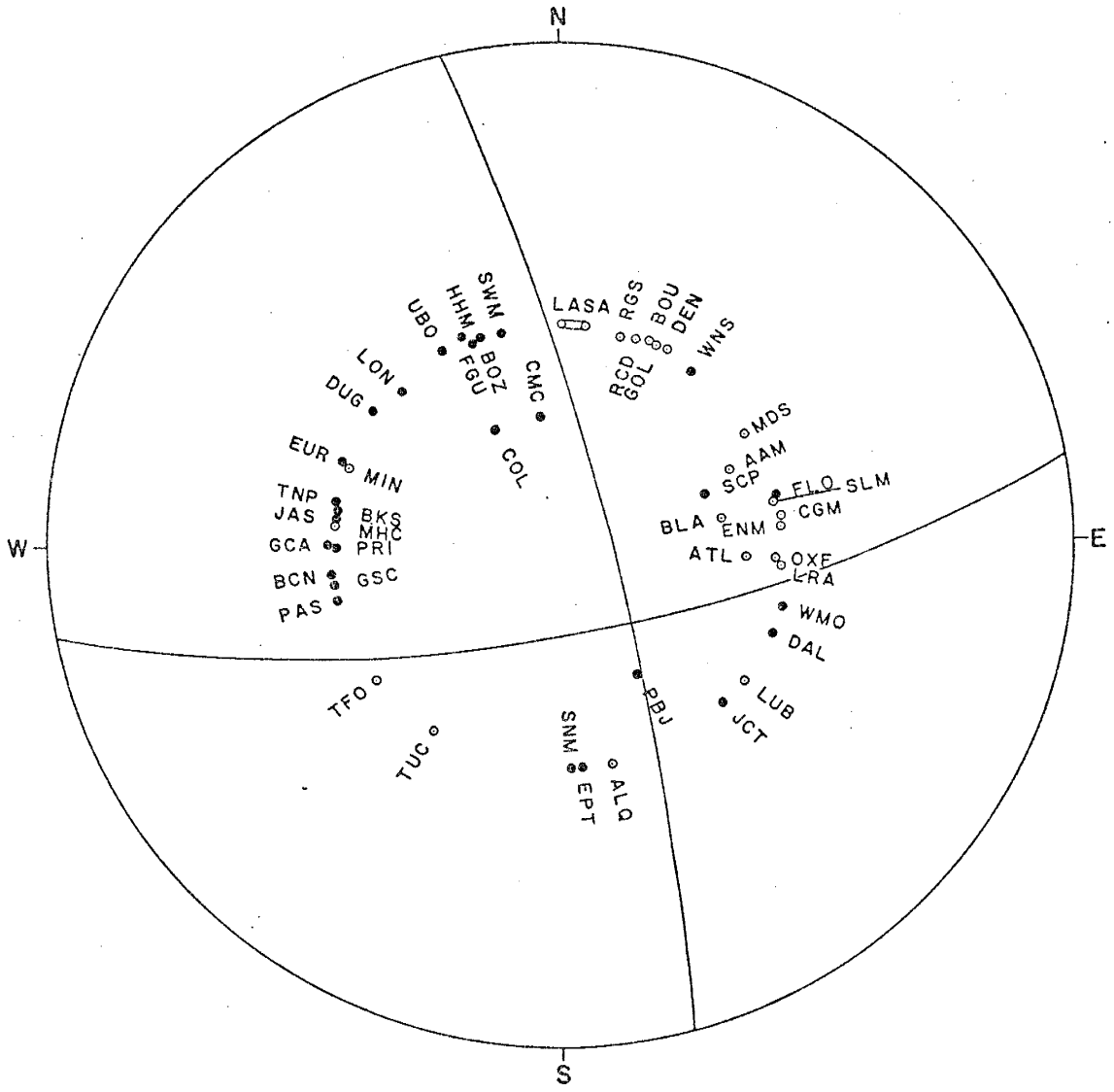

Figure 3-5. Focal mechanism diagram based on first motion of P waves on short-period instruments at all stations.

overwhelming predominance of compressions in the general northwest direction from the epicenter, between PAS and SWM. From LASA, representing the data of 19 stations, to DEN evidence of dilatational first motions is convincing. Dilatational first motion continues, although less convincingly, clockwise to about due east at LRA. From that point on, the data are not very meaningful until ALQ is reached. For the most part, stations at azimuths between 35° and 160° tell us little. However, ENM and WMO were rated as good ("G" in Table 3-1) in the quality of their first motions and show opposite directions of first motion suggesting a nodal plane may pass between them. This conclusion is also supported by JCT, which has a first motion rated good.

From ALQ to TFO, evidence of dilatational first motions is good. EPT and SNM have first motions of poor quality. Such "emergent" phases as this were a source of difficulty in the interpretation of a large number of the available seismograms. On the other hand, ALQ and TUC were very obvious dilatations and were rated very good ("VG").

To summarize the evidence of Figure 3-5 in a rather general way, the approximate distributions of first motions with azimuth are:

(1) compressings, 250° to 350°;

(2) dilatations, 0° to 100°;

(3) compressions, 100° to 140°;

(4) dilatations, 160° to 240°.

A set of nodal planes has been drawn on Figure 3-5 corresponding to the above distribution of first motions. Besides being consistent with the patterns of first motions, a requirement of the nodal planes is that they must be perpendicular to each other. On the Wulff net, this requires that the line representing each plane pass through the point corresponding to the pole of the other plane. It should also be pointed out here that the direction of motion on a fault is normal to the auxiliary plane and therefore is represented on the stereographic projection by the pole of the auxiliary plane.

Figure 3-6 shows the distribution obtained by using only first motions rated as good or very good. In this case the divisions of the stereographic projection into four parts is quite clear. The dashed lines represent the limits of the positions of the lines representing the nodal planes. Each solid line, A or B, represents a plane having the median values of strike and dip between the corresponding limits.

Interpretation.

Without further evidence, such as that based on S polarization data, the decision as to which nodal plane represents the fault can not be made. However, in view of Figure 3-6, two interpretations are possible:

(1) Plane A is a right-lateral strike-slip fault, striking N18^{o}W and dipping 79^{o} ENE, with a direction

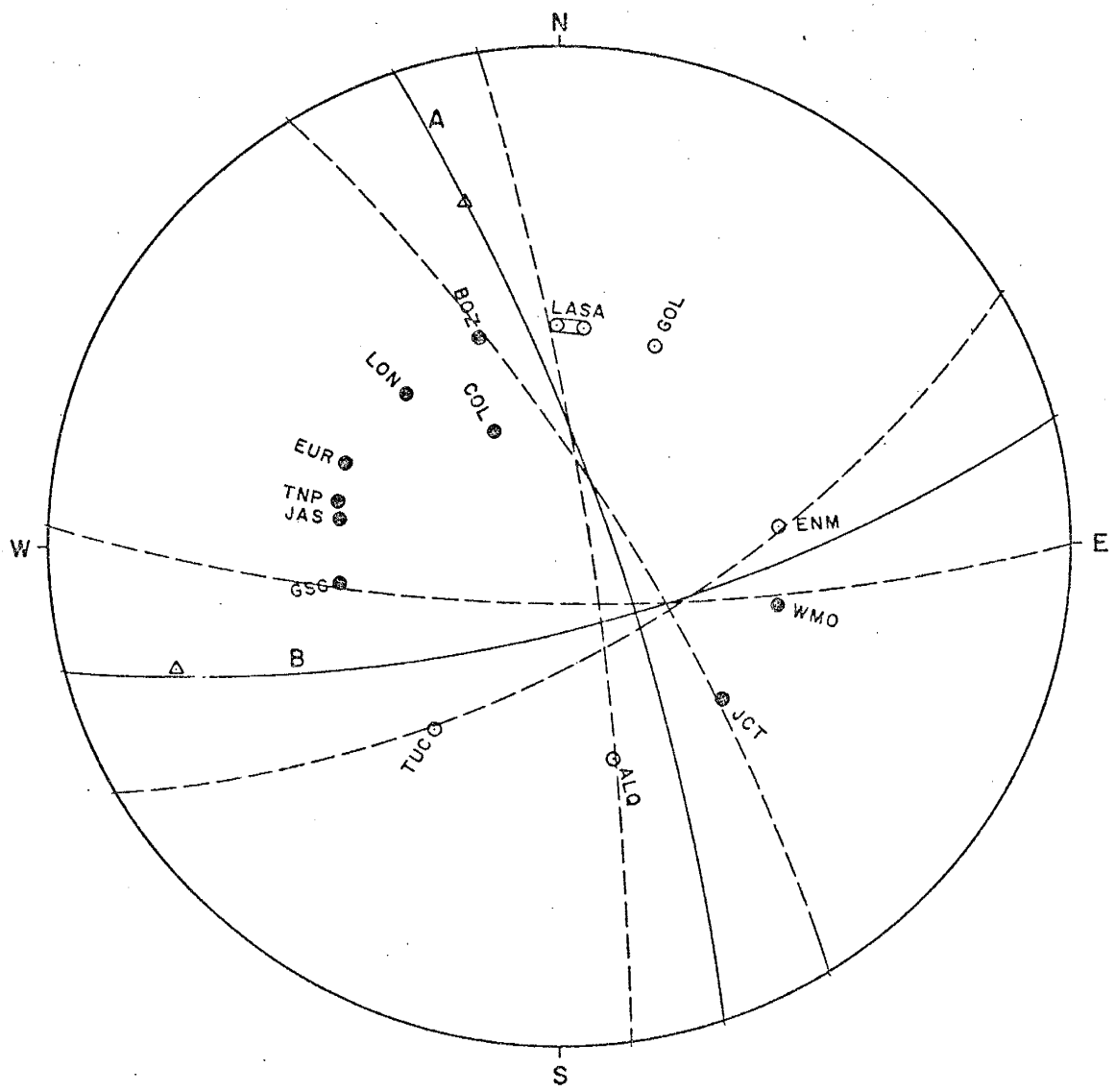

Figure 3-6. Focal mechanism diagram based on first motion of P waves on short-period instruments on the seismograms which are rated as either G (good) or VG (very good).

of motion at N14°W, plunging 20°;

(2) Plane B is a left-lateral strike-slip fault, striking N76°E and dipping 70° SSE, with a direction of motion at N72°E, plunging 12°.

Discussion

The geology of the Dulce area can be used to eliminate the ambiguity in the focal mechanism solution. First, there is the evidence of late Miocene faulting (see Figure 2-6). The geologic maps (Dane, 1948; Bingler, 1968) show that these faults, in the epicentral region, strike from N20°W to N35°W. In addition, the dense series of lamprophyre dikes of Miocene age trend almost due north-south. The dikes are thought to be slightly older than the faults, according to Dane. This writer did not observe any evidence of more recent faulting in the field.

Although at least one of the faults shows a good deal of vertical displacement, either of the sets of dislocation surfaces, the faults or the dikes, could influence the orientation of the plane of contemporary faulting by providing planes of weakness along which the latter can occur. In that case a north to northwest striking fault would be a good possibility.

In terms of principal stresses, a strike-slip fault striking north-northwest would require a least principal stress with a generally east-west axis. This orientation is

consistent with the north-south trending dikes and with the tectonic origin of the Rio Grande rift to the east. Therefore, a fault along plane A seems the more probable.

4. MAGNITUDE

Introduction

Magnitudes of the earthquake at Dulce and the nuclear explosion, Gasbuggy, were determined by the U. S. Coast and Geodetic Survey and by Reagor, et al. (1968). However, comparisons of magnitudes between the two events is difficult because different formulas were used in the determinations. The purpose in repeating the determinations in this study was to assure that the same techniques were applied in evaluating the magnitudes of both events in order to obtain the best possible comparison.

Three magnitudes were calculated for each event: (1) a magnitude based on the refracted P phase, called m; (2) a magnitude based on the direct P phase (Pg), called m_6; and (3) a magnitude based on Rayleigh waves, called M_s. All formulas used were of the form,

$$m \text{ (or } M_s) = K_1 \log \Delta + K_2 \log (A/T) + K_3, \qquad (4\text{-}1)$$

where Δ is distance, A ground amplitude, and T period. The units of Δ and A depend on the formula used. Only seismographs yielding good seismograms for both events were used in the calculations.

Magnitude Determinations

Magnitudes from the Refracted P Phase.

The magnitude based on refracted P waves is determined by one of three formulas, depending on the distance range:

$$m = 3.68 \log \Delta + 1.21 \log (A/T) - 7.55,$$

(0 to 1000 kilometers); (4-2)

$$m = 2.00 \log \Delta + 1.00 \log (A/T) - 3.27,$$

(1000 to 1800 kilometers); (4-3)

$$m = 4.00 \log \Delta + 1.00 \log (A/T) - 10.35,$$

(beyond 1800 kilometers); (4-4)

where Δ is measured in kilometers, A in millimicrons and T in seconds (Evernden, 1967). Amplitude A is the maximum peak-to-peak ground amplitude in the first six oscillations of the refracted P phase. Three formulas are necessary because refracting layers within the crust and upper mantle lead to three different first arrivals depending on the distance from the source.

The magnitudes, m, calculated from the refracted P phase, are listed in Table 4-1. An interesting result is the close agreement between the magnitudes for the earthquake and Gasbuggy. Each event has a mean value of 5.1 with a calculated standard deviation of about 0.5. The standard deviation of the magnitudes for each event indicates that the magnitudes of the two events could differ by several tenths of a unit magnitude. However, an examination of the fourth column of the table reveals that, except for two stations, the difference in magnitudes is quite small between events at every station. The standard deviation of these difference values is only 0.3, mostly contributed by the large values for DUG and GSC.

Table 4-1. Magnitudes from the Refracted P Phase.

Station	m(e) (earthquake)	m(n) (Gasbuggy)	m(e) - m(n)
AAM	4.8	5.1	-0.3
BOZ	4.7	4.6	0.1
DAL	5.0	4.9	0.1
DUG	4.6	5.2	-0.6
GSC	6.2	5.6	0.6
LUB	4.8	4.7	0.1
RCD	5.9	6.0	-0.1
TUC	4.8	4.7	0.1
AVERAGES	5.1 $\pm$ 0.6	5.1 $\pm$ 0.5	0.0 $\pm$ 0.3

Magnitudes from the Direct P Phase.

The magnitude based on direct P waves employs the formula,

$$m_6 = 3.42 \log \Delta + 1.14 \log (A/T) - 8.00, \qquad (4\text{-}5)$$

where Δ is measured in kilometers, A in millimicrons, and T in seconds (Evernden, 1967). The amplitude A is the maximum peak-to-peak ground amplitude in the P_g phase. The direct P phase, Pg, was not the first arrival at any of the stations used, and in this case only four stations yielded good data for both events.

Table 4-2 is a list of the values of m_6. The standard deviation for the differences between the magnitudes of the two events is only 0.1.

Another interesting result is the large differences in the magnitudes m_6. The mean value of the difference is 0.6, compared to a mean difference of 0.0 for magnitudes based on the refracted P phase. Therefore, the earthquake at Dulce radiated a much greater relative amount of energy into the direct P phase than did Gasbuggy. This difference can be explained in terms of source mechanism. If the earthquake originates on a vertical strike-slip fault, the direction of most intense P wave radiation is horizontal. The direct P phase is relatively large compared to the refracted P phase. On the other hand, the nuclear explosion is likely to have a nearly spherical radiation pattern. In the latter case, the refracted P phase is expected to be relatively large compared to the direct P phase.

Table 4-2. Magnitudes from the Direct P Phase.

Station	m_6(e) (earthquake)	m_6(n) (Gasbuggy)	m_6(e) - m_6(n)
BOZ	4.6	3.9	0.7
GSC	5.7	5.2	0.5
LUB	5.2	4.5	0.7
RCD	5.6	5.0	0.6
AVERAGES	5.3 $\pm$ 0.4	4.6 $\pm$ 0.4	0.6 $\pm$ 0.1

Magnitude from Surface (Rayleigh) Waves.

The magnitude, M_S, from Rayleigh waves, is determined from the formula,

$$M_S = 1.66 \log \Delta - 1.00 \log (A/T) - 3.30, \qquad (4\text{-}6)$$

where Δ is measured in degrees, A in microns, and T in seconds (Reagor et al., 1968). In this formula, A should be the peak-to-peak amplitude of the 20-second Rayleigh wave. However, Reagor et al. noted "that the formula applies to other wave periods as well when the measurements of A/T are associated with maximum amplitudes." Therefore, in this dissertation, the maximum peak-to-peak ground motion in the Rayleigh wave was used. On most of the seismograms, the maximum Rayleigh pulse was also the first and longest-period Rayleigh wave and had a period of from 14 to 17 seconds.

The magnitudes, M_S, are listed in Table 4-3. As was the case for the previous two magnitude results, based on P waves, the scatter found in the calculated values of M_S for each event was larger than the scatter obtained in subtracting the magnitudes for Gasbuggy from those for the earthquake. And, as was the case for m_6, the mean difference is 0.6. This indicates that the earthquake was a stronger generator of surface waves than the nuclear explosion.

Table 4-3. Magnitudes from Surface Waves.

Station	$M_S(e)$ (earthquake)	$M_S(n)$ (Gasbuggy)	$M_S(e) - M_S(n)$
ALQ	4.1	3.4	0.7
ATL	5.2	4.8	0.4
DAL	5.1	4.5	0.6
DUG	4.8	4.2	0.6
GOL	4.7	3.9	0.8
GSC	5.3	4.6	0.7
LON	4.7	4.6	0.1
LUB	4.8	4.3	0.7
OXF	5.0	4.2	0.8
SLM	5.5	4.9	0.6
TUC	4.8	4.1	0.7
AVERAGES	4.9 ± 0.4	4.3 ± 0.4	0.6 ± 0.2

Discussion

Variation of Magnitude with Azimuth.

Figure 4-1 is a graph of the magnitude m as a function of station azimuth. No convincing variation is magnitude with azimuth is seen. Lee and Borcherdt (1968) studied the peaks in the power spectral density of Gasbuggy and found that, at distances up to 500 kilometers, the greatest amount of energy was radiated to the west and southwest of Gasbuggy. They also found that, at distances less than 400 kilometers, the radiation to the north was high, which agrees with the values obtained at two stations in Figure 4-1 at azimuths of 21° (RCD) and 260° (GSC), respectively. The distances of these two stations, about 900 kilometers, however, were considerably greater than 400 kilometers.

Figure 4-2 is a graph of the magnitude M_S as a function of station azimuth. The magnitudes appear to peak at azimuths of 80° and 260° for both the earthquake and the nuclear explosion. Such an azimuthal variation in energy radiation by surface waves is most likely to be the result of crustal and upper mantle structure. However, another possibility is that Gasbuggy released tectonic strain energy. Both events could have occurred in the same stress environment. Archambeau and Sammis (1970) show that the Rayleigh wave radiation from the nuclear explosion Bilby had a two-lobed pattern, similar to that obtained for Gasbuggy. The radiation pattern they obtained agrees in shape and

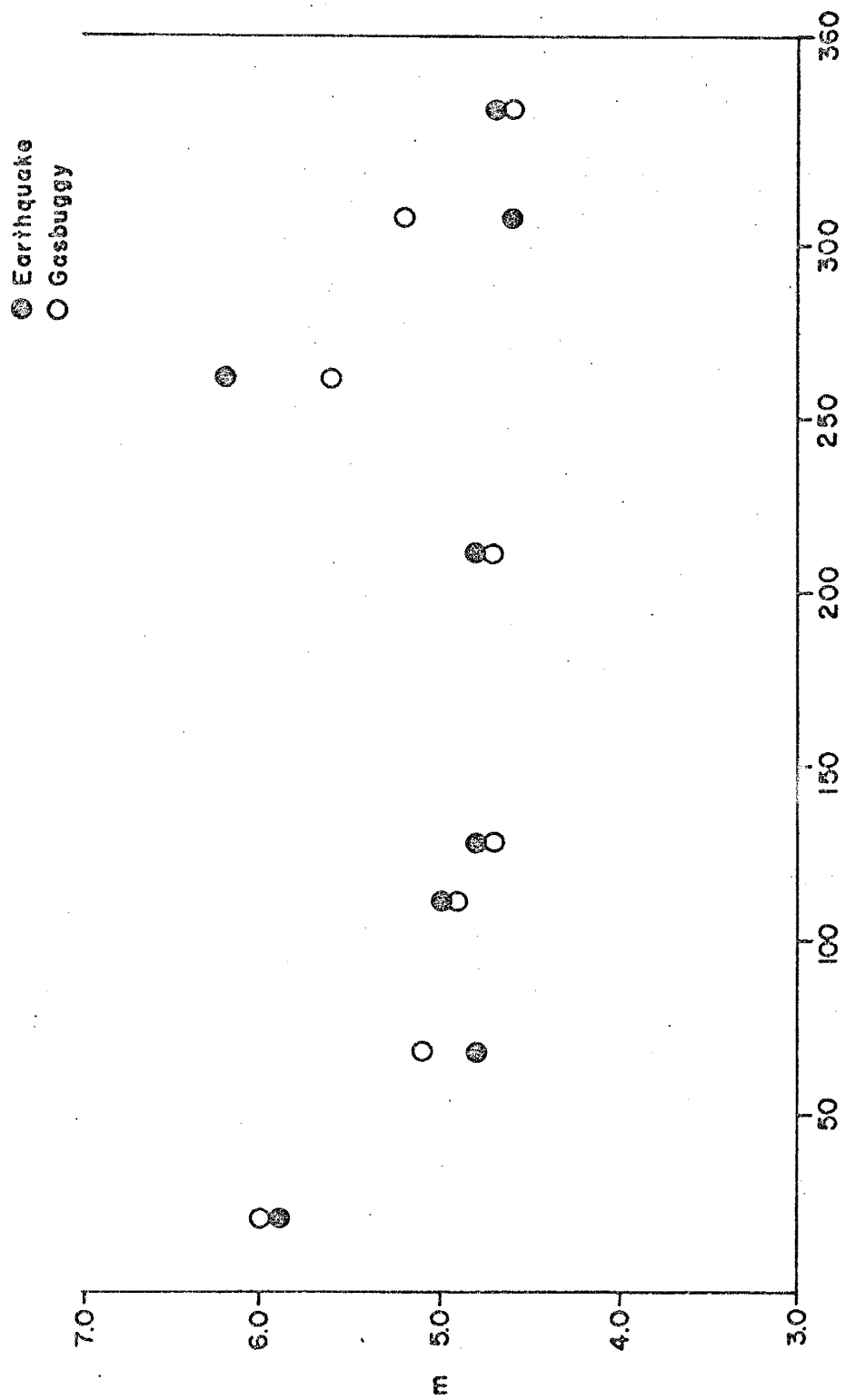

Figure 4-1. The magnitude m as a function of azimuth for the Dulce earthquake and Gasbuggy.

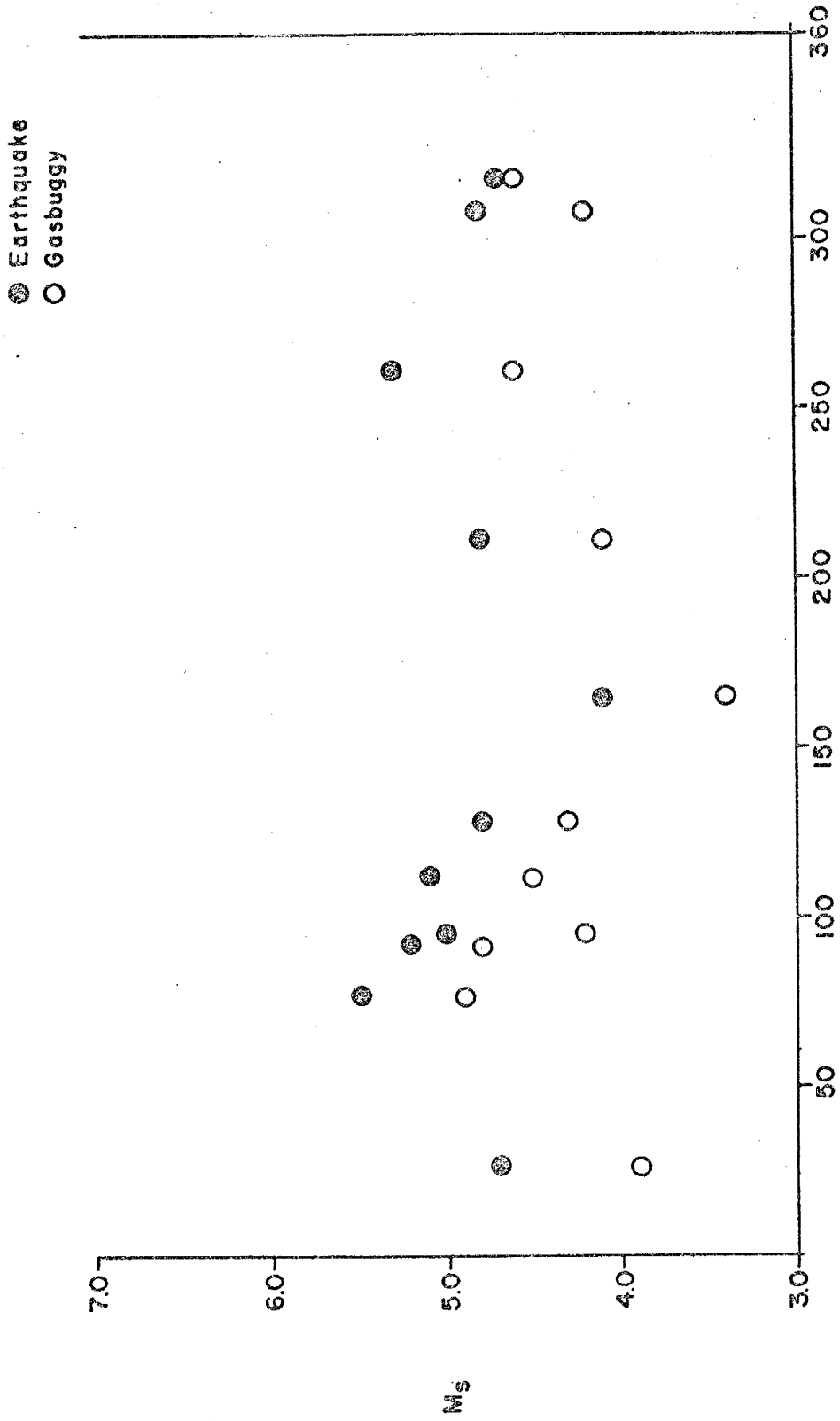

Figure 4-2. The magnitude Ms as a function of azimuth for the Dulce earthquake and Gasbuggy.

orientation with that theoretically predicted for a nuclear explosion in a pre-stressed medium. The theoretical prediction is based on a model in which the radiation from an explosion is superimposed on the radiation from a double couple source. The latter represents energy released from a pre-existing tectonic shear stress field in the medium. However, release of tectonic stress is not a probable explanation for the distribution of Gasbuggy magnitudes because energies calculated from the magnitudes indicate that radiation in the east and west directions was about 1000 times that in the north and south directions.

The most important observation of this section is that the variations in a single type of calculated magnitude can not be explained in terms of source mechanism. The two events are quite different in this respect, yet produce the same radiation pattern. Apparently, therefore, the observed variations in a particular magnitude from station to station are independent of the source and arise from variations in crustal and mantle structure.

Variations between m, m_6, and M_s.

A comparison of the different types of magnitude for the two events confirms the difference in source mechanism between an earthquake and a nuclear explosion. For the earthquake, $m_6 > m > M_s$; for Gasbuggy, $m > m_6 > M_s$. Comparing the two events, the magnitudes m are equal, but m_6 and

M_S are considerably greater for the earthquake than for Gasbuggy.

The latter observation is in agreement with the work of other researchers. The relation between m and M_S for earthquakes has been investigated by Gutenberg and Richter (1956) and found to be

$$M_S = 1.59\ m - 3.97. \qquad (4\text{-}7)$$

A similar relation has been established by Thirlaway and Carpenter for a nuclear explosion (Liebermann and Pomeroy, 1969):

$$M_S = m - 1.8. \qquad (4\text{-}8)$$

Letting m = 5.1, which is the magnitude found in this paper for both events, the values of M_S (by equations 4-7 and 4-8) for the earthquake and explosion are, respectively, 4.1 and 3.3. The corresponding values of M_S reported in this paper are 4.9 and 4.3, which exceed those from the formulas by 0.8 and 1.0, respectively. According to Liebermann and Pomeroy (1969) such deviations from the formulas are to be expected for events in the Western United States. In their paper, the magnitudes of several earthquakes and nuclear explosions of the Western United States were examined, with the result that, for magnitude m = 5.1, earthquakes and nuclear explosions of that geographical area do indeed have values of M_S which exceed those predicted from the formulas by about 0.8 and 1.1, respectively.

Although no magnitude calculations based on S wave radiation are made, an important visual observation is made. Whereas the earthquake produced a very large-amplitude SH phase, SH was virtually absent for Gasbuggy. This observation is not surprising and it confirms the expected differences between earthquake and explosive sources.

Magnitude and Yield of Gasbuggy.

The magnitude m = 5.1 for Gasbuggy is consistent with known yield-magnitude relations. Evernden (1970) displays on a graph the magnitude of nuclear explosions as a function of yield for a number of geologic environments. Gasbuggy was detonated in a shale environment and had a yield of 26 kilotons. According to Evernden's graph, a 26 kiloton shot in "hard rock" would have a magnitude of about m = 5.1, the same value as is found for Gasbuggy.

5. SOURCE PARAMETERS

Introduction

In this section the source parameters for the Dulce earthquake and Gasbuggy are discussed. The parameters considered are the time durations and linear source dimensions of the sources, and the fault displacement of the earthquake.

Time Durations of the Sources

The durations of the earthquake and Gasbuggy were determined from the ratio of the amplitude spectra of the two events using a method similar to that of Davies and Smith (1968). The technique was to form the ratio of the absolute values of the amplitude spectra of the P phase on long-period records of the nuclear explosion and the earthquake. By taking the spectral ratio, the effects of path and the effects of digitizing, truncation of digital data, and so on, were removed. For comparable release of P wave energy, an earthquake is expected to have a considerably larger time duration than a nuclear explosion. Separately, the amplitude spectra contain information about the source time durations. Because the durations are different, the spectral ratio should preserve this information. Therefore, two dominant quefrencies* are expected in the spectral ratio: one equal

* "Quefrency" is the term applied to the number of peaks per unit frequency interval in the amplitude spectrum;

to the duration of the earthquake and one equal to the duration of the nuclear explosion.

The first eight seconds of the P phase on long-period (30-second) vertical component records were used in this analysis. The spectral ratios showed fairly regular sets of ripples for records from two seismograph stations, DUG and GSC. Quefrencies of 0.5 second and 1.8 seconds were observed in the spectral ratio based on DUG seismograms (see Figure 5-1). These probably represent the duration of the nuclear explosion and the duration of the earthquake, respectively. The corresponding values for station GSC were 0.4 second and 1.7 seconds.

These values can be compared to those found by Davies and Smith (1968). Their study yielded a duration of 0.4 seconds for the Shoal nuclear explosion, which had a body wave magnitude of 4.9 (compared to 5.1 for Gasbuggy), and a duration of 2.4 seconds for the Fallon earthquake, which had a body wave magnitude of 4.4 (compared to 5.1 for the Dulce shock. In what follows, the durations of Gasbuggy and the earthquake at Dulce are taken to be 0.5 second and 1.8 seconds, respectively, although the latter value may be too small.

quefrency, in the frequency domain, corresponds to frequency in the time domain.

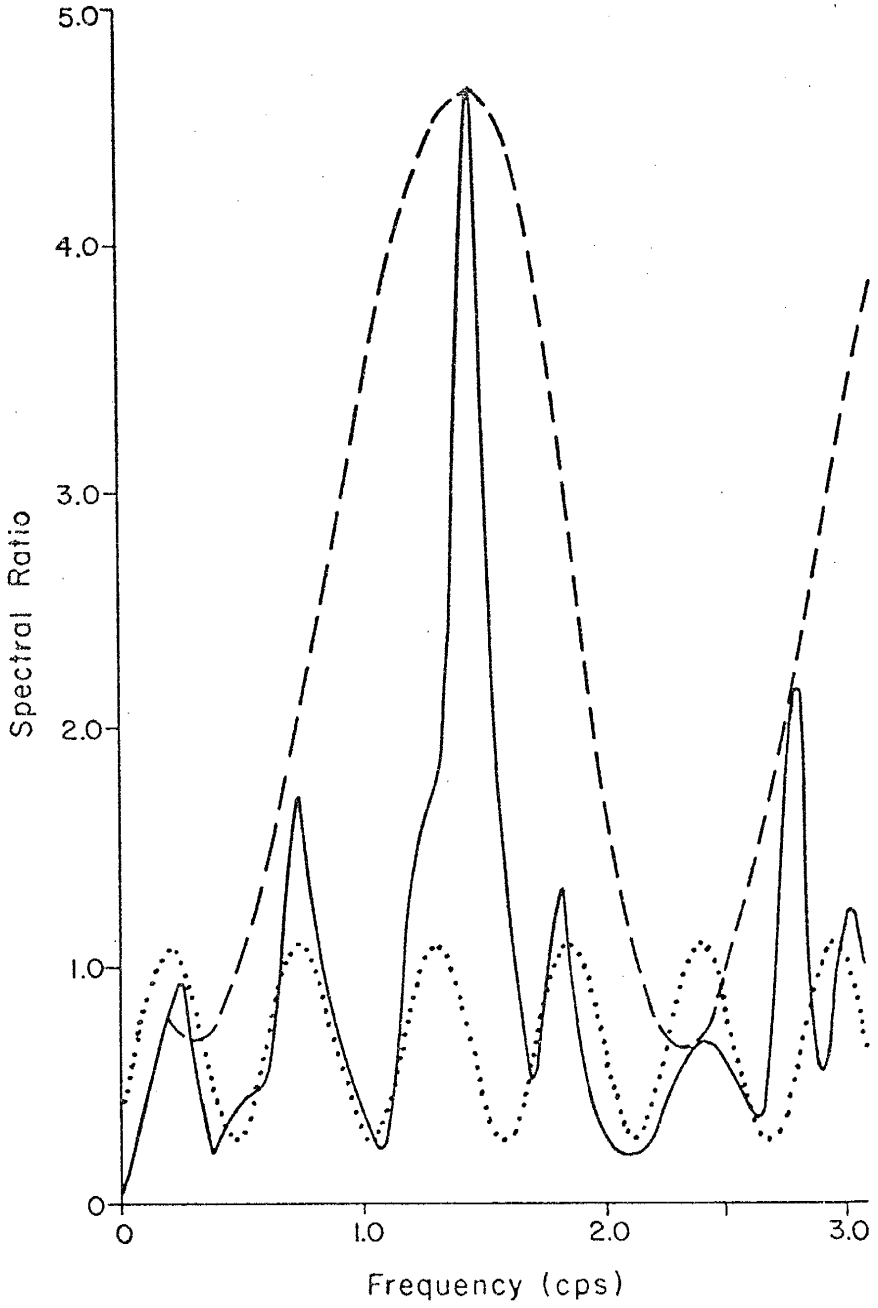

Figure 5-1. Ratio of the amplitude spectra (solid line) of the Dulce earthquake and Gasbuggy from seismograph station DUG. Reference curves are superposed which correspond to quefrencies of 0.5 sec (dashed line) and 1.8 sec (dotted line).

Linear Dimensions of the Sources

Dimensions from Time Durations.

Gasbuggy was detonated at a depth of 1.26 kilometers near the top of the 600 meter-thick Lewis Shale (Dane, 1948). The detonation point is overlain by about 900 meters of sandstones, shales, and clays, mostly of the Animas Formation. A reasonable P wave velocity for these rocks is 2.0 km/sec (Grant and West, 1965). The inelastic zone surrounding the explosion is assumed to form at about 0.75 P wave velocity of the medium (Davies and Smith, 1968). Combining the velocity of 1.5 km/sec with a rupture duration of 0.5 second, yields a radius for the inelastic rupture zone of 0.75 kilometer.

The depth of focus of the earthquake was probably not more than about 12 kilometers. This estimate is based on the maximum possible depth of the aftershocks. Three portable seismograph units were placed around the Dulce area within a few days after the main shock by personnel of the U. S. Coast and Geodetic Survey's seismological observatory at Albuquerque (Werner and Hoffman, unpublished report). One of these stations was located for a time at the town of Dulce and the calculated P - O intervals from that unit for seven of the largest aftershocks ranged from 1.0 second to 1.7 seconds. This yields a maximum possible depth for the aftershocks of 10 kilometers, assuming an average P wave velocity of 6 km/sec. Therefore, the focus of the main

shock must have been within the crust where a P wave velocity of 6 km/sec is reasonable.

An earthquake fault is believed to rupture with a velocity approximately equal to the shear wave velocity (Press, et al., 1961; Khattri, 1969). Consequently, the velocity of rupture propagation is $V_S = 6 / 1.73 = 3.5$ km/sec. Combining this velocity with the duration of 1.8 seconds yields a fault length of 6.3 kilometers for a unilaterally propagating fracture and 12.6 kilometers for a bilateral fault.

Dimensions from Magnitudes.

Attempts have been made by several researchers to relate earthquake magnitude to source dimension. In particular, Liebermann and Pomeroy (1970) demonstrate that in the magnitude range 3 to 6 the formula,

$$m = 2.8 + 1.9 \log A^{\frac{1}{2}}, \qquad (5\text{-}1)$$

is applicable, where A is the fault area in square kilometers. For $m = 5.1$ this formula yields $A^{\frac{1}{2}} = 16$ kilometers.

In the same paper, Liebermann and Pomeroy tabulate the magnitudes and diameters of the rupture zones of five nuclear explosions. Although no formula can be applied, due to the few data available, the values given suggest that the diameter corresponding to $m = 5.1$ would be around 1.5 kilometers. Therefore the radius of the zone of inelastic deformation for Gasbuggy would be around 0.75 kilometers.

Dimensions from Surface Waves.

An analogy to antenna theory has been applied to earthquake sources by Liebermann and Pomeroy (1969). In their paper, it is stated that Keylis-Borok has shown that the most efficient generation of surface waves is at wavelengths four times the dimension of the source. Rayleigh wave records from the Dulce earthquake usually show a maximum at periods around 15 seconds. Using a Rayleigh wave velocity of 3.2 km/sec the resulting wavelength is 48 kilometers. This yields a fault length of 12 kilometers, considering the fault as a quarter-wavelength antenna.

Fault Displacement of the Earthquake

An estimate of the expected displacement of an earthquake of this magnitude can be obtained from

$$\log(LD^2) = 2.24\ M_s - 4.99, \qquad (5\text{-}2)$$

where L is the fault length and D the displacement (King and Knopoff, 1968). This equation is based on earthquakes of magnitudes $M_s > 5.5$. However the Dulce magnitude is not too much less than this and the application of the formula should give a good approximate value. Letting L = 10 kilometers and $M_s = 4.9$, the resulting displacement is 1.0 centimeter. Even if this earthquake's fault extends to the surface, visible surface features would be very difficult to find.

Conclusions

The type of calculations performed in this section are not very exacting. Nevertheless, it is felt that the values obtained are much better than "order of magnitude" calculations because the results obtained are consistent with each other and with the work of other authors to within a factor of two or so.

In summary, the Dulce shock had approximately the following source parameters: depth, 10 kilometers; duration, 1.8 seconds; fault length, 10 kilometers; displacement, 1 centimeter. For Gasbuggy the parameters were approximately as follows: depth, 1.3 kilometers; duration, 0.5 second; radius of rupture zone, 0.75 kilometer.

SUMMARY

The Dulce, New Mexico, earthquake of January 23, 1966, occurred at 01h 56m 39.3s GMT. The epicenter was located at 36.96° north latitude and 106.95° west longitude, and the focal depth was about 10 kilometers. The earthquake was the result of right-lateral strike-slip movement along a fault having a strike of N18°W and a dip of 79° ENE. The duration of the fault motion was 1.8 seconds, the fault length was about 10 kilometers, and the displacement was approximately 1 centimeter directed N14°W and plunging 20°. The average calculated values of the magnitudes were as follows: the magnitude from the refracted P phase, m = 5.1; the magnitude from the direct P phase, m_6 = 5.3; and the magnitude from surface waves, M_S = 4.9.

The nuclear explosion, Gasbuggy, was detonated on December 10, 1967, at 19h 30m 00.1s GMT. The geographic coordinates were 36.68° north latitude and 107.21° west longitude, and the depth of the shot was 1.26 kilometers. The zone of inelastic deformation had a radius of 0.75 kilometers and was formed in 0.5 seconds. The yield of Gasbuggy was 26 kilotons. The average calculated values of its magnitudes were as follows: the magnitude from the refracted P phase, m = 5.1; the magnitude from the direct P phase, m_6 = 4.6; and the magnitude from surface (Rayleigh) waves, M_S = 4.3.

The value of m was the same for both events, but m_6 and M_S were considerably larger for the earthquake than for the nuclear explosion. This difference reflects the difference in the source mechanisms and lends support to the strike-slip mechanism for the earthquake. The variation in the values of each type of magnitude from station to station was the same for both events. Therefore, the scatter in the calculated magnitude values for both seismic events was probably the result of variations in crustal and upper mantle structure.

The study of the Dulce earthquake turned out to be more difficult than originally anticipated. Although other investigators have had reasonable success with events having magnitudes (m_b) as low as 5.5 in other areas of the world, apparently this is not likely to be the case for a shock located in the western United States. A number of the stations relatively close to the epicenter had fairly obscure first arrivals. A greater number of stations closer to the epicenter would have improved the analysis substantially.

Despite the difficulties, studies of events like the Dulce shock are of considerable value. Earthquakes of this magnitude are relatively rare in the interior of the tectonic plates. The results of this study may eventually help to determine the nature of the stress distributions within the North American plate and/or along the boundaries of the smaller segments which comprise the North American plate.

REFERENCES CITED

Albuquerque Journal (1950). From the column, "50 years ago," May 4, 1950, issue, Albuquerque Journal, Albuquerque, New Mexico.

Archambeau, C. and C. Sammis (1970). Seismic radiation from explosions in prestressed media and the measurement of tectonic stress in the earth, Rev. Geophys. 8, 473-499.

Banghar, A. R. and L. R. Sykes (1969). Focal mechanisms of earthquakes in the Indian Ocean and adjacent regions, J. Geophys. Research 74, 632-649.

Bingler, E. C. (1968). Geology and Mineral Resources of Rio Arriba County, New Mexico, New Mexico Institute of Mining and Technology, State Bureau of Mines and Mineral Resources, Socorro, New Mexico, Bulletin 91, 158 p.

Dane, C. H. (1948). Geologic Map of Part of Eastern San Juan Basin, Rio Arriba County, New Mexico, U. S. Geological Survey, Oil and Gas Inv. Prelim. Map 78.

Davies, J. B. and S. W. Smith (1968). Source parameters of earthquakes, and discrimination between earthquakes and nuclear explosions, Bull. Seism. Soc. Am. 58, 1503-1517.

Engdahl, E. R. and R. H. Gunst (1966). Use of a high speed computer for the preliminary determination of earthquake hypocenters, Bull. Seism. Soc. Am. 56, 325-336.

Evans, D. M. (1966). Man-made earthquakes in Denver, Geotimes 10:9, 11-18.

Evernden, J. F. (1967). Magnitude determination at regional and near-regional distances in the United States, Bull. Seism. Soc. Am. 57, 591-639.

Evernden, J. F. (1970). Magnitude versus yield of explosions, J. Geophys. Research 75, 1028-1032.

Grant, F. S. and G. F. West (1965). Interpretation Theory in Applied Geophysics, McGraw-Hill Book Company, 583 p.

Gutenberg, B. and C. F. Richter (1956). Magnitude and energy of earthquakes, Annali Geofisica 9, 1-15.

Herrin, E. et al. (1968). 1968 seismological tables for P phases, Bull. Seism. Soc. Am. 58, 1193-1241.

Isacks, B., J. Oliver, and L. R. Sykes (1968). Seismology and the new global tectonics, J. Geophys. Research 73, 5855-5899.

Khattri, K. N. (1969). Determination of earthquake fault plane, fault area, and rupture velocity from the spectra of long period P waves and the amplitude of SH waves, Bull. Seism. Soc. Am. 59, 615-630.

King, C.-Y. and L. Knopoff (1968). Stress drop in earthquakes, Bull. Seism. Soc. Am. 58, 249-257.

Lee, W. H. K. and R. D. Borcherdt (1968). Pn Spectral Variations of the Gasbuggy Explosion at Intermediate Distance Ranges, U. S. Geological Survey, Tech. Letter NCER-9, open file report, 18 p.

Liebermann, R. C. and P. W. Pomeroy (1969). Relative excitation of surface waves by earthquakes and underground explosions, J. Geophys. Research 74, 1575-1590.

Liebermann, R. C. and P. W. Pomeroy (1970). Source dimensions of small earthquakes as determined from the size of the aftershock zone, Bull. Seism. Soc. Am. 60, 879-890.

Press, F., A. Ben-Menahem, and M. N. Toksoz (1961) Experimental determination of earthquake fault length and rupture velocity, J. Geophys. Res. 66, 3471-3485.

Ramsay, J. G. (1967). Folding and Fracturing of Rocks, McGraw-Hill Book Company, 568 p.

Reagor, B. G., D. W. Gordon, and J. N. Jordan (1968). Seismic Analysis of a Nuclear Explosion: Gasbuggy, U. S. Coast and Geodetic Survey, Seismology Division, Washington, D. C., 73 p.

Richter, C. F. (1958). Elementary Seismology, W. H. Freeman and Co., 768 p.

Richter, C. F. (1959). Seismic regionalization, Bull. Seism. Soc. Am. 49, 123-162.

Sanford, A. R. (1963). Seismic activity near Socorro, N. Mex. Geol. Soc., Guidebook, 14th Field Conf., p. 146.

Sanford, A. R. (1965). An Instrumental Study of New Mexico Earthquakes, New Mexico Institute of Mining and Technology, State Bureau of Mines and Mineral Resources, Socorro, New Mexico, Circular 78, 12 p.

Sanford, A. R. and D. J. Cash (1969). An Instrumental Study of New Mexico Earthquakes, July 1, 1964, through December 31, 1967, New Mexico Institute of Mining and Technology, State Bureau of Mines and Mineral Resources, Socorro, New Mexico, Circular 102, 7 p.

Simon, R. (1969). Seismicity of Colorado: consistency of recent earthquakes with those of historical record, Science 165, 897-899.

Stauder, W. J. (1962). The focal mechanism of earthquakes, Adv. in Geophysics 9, 1-76.

Steinbrugge, K. V., W. K. Cloud, and N. H. Scott (1970). The Santa Rosa, California, Earthquakes of October 1, 1969, U. S. Coast and Geodetic Survey, Washington, D. C.

Sykes, L. R. (1967). Mechanism of earthquakes and nature of faulting on the mid-oceanic ridges, J. Geophys. Research 72, 2131-2153.

Von Hake, C. A. and W. K. Cloud (1968). United States Earthquakes, 1966, U. S. Coast and Geodetic Survey, Washington, D. C.

This thesis is accepted on behalf of the faculty of the Institute by the following committee:

Allan R. Sanford

A. T. Rudolph

Alan Shanthes.

Leslie O. Fallon

Date May 10, 1971